12-2018

Dimensional Analysis and Variational Formulation of Diffuse Optical Tomography (DOT) Model

Thowhida Akther
Clemson University, takther@clemson.edu

Dimensional Analysis and Variational formulation of Diffuse Optical Tomography (DOT) Model

---

A Thesis
Presented to
the Graduate School of
Clemson University

In Partial Fulfillment
of the Requirements for the Degree
Master of Science
Mathematics

---

by
Thowhida Akther
December 2018

Accepted by:
Dr. Taufiquar R. Khan, Committee Chair
Dr. Hyesuk Lee
Dr. Shitao Liu

Abstract

Diffuse Optical Tomography (DOT) is an emerging modality for soft tissue imaging with medical applications including breast cancer detection. DOT has many benefits, including its use of non ionizing radiation and its ability to produce high contrast images. However, it is well known that DOT image reconstruction is unstable and has low resolution. DOT uses near infra-red light waves to probe inside a body; for example, DOT can be used to measure the changes in the amount of oxygen in tissues, which can detect early stages of cancer in soft tissues such as the breast and brain. In this thesis, we perform dimensional analysis to obtain a dimensionless form of the ODE for the 1-d DOT model and the PDE for the 2-d DOT model. We later solve the 1-d cases using the finite element method (FEM) in MATLAB. We investigate whether the inverse problem using the dimensionless scaled forward DOT model will improve the ill-posedness of the image reconstruction problem in the 1-d case. We solve the inverse problem for DOT image reconstruction by reformulating the inverse problem as a variationally constrained non-linear optimization problem and compare solving the optimization problem for specific cases of the 1-d DOT model with Newton's iteration versus the traditional Gauss-Newton method. We observe the effects of different regularization parameters and step lengths on the reconstructions for Newton's iteration. We also observe the effect of moving the inclusion away from the boundary during image reconstruction. Using the optimally derived regularization

parameter from the noise-free data, we reconstructed the parameter space by adding different levels of noise to the synthetic data. Based on our simulations in 1-d, we conclude that the scaled inverse problem is still ill-posed but that the variational approach provides a better reconstruction than the Gauss-Newton method.

Dedication

To the Almighty Allah, my beloved parents, my dearest husband and my apple of eyes, my daughter.

Acknowledgments

First of all, I would like to thank Almighty Allah who gives me the capability and strength to fulfill my long-cherished dream of earning a higher degree from abroad, especially from the United States of America.

I would like to express my special thanks of gratitude to my advisor, Dr. Taufiquar Khan, who advised me since my first year at Clemson. His guidance helped me in all the time of research and writing of this thesis. He was always confident in my abilities, encouraged me to pursue my passions, and do what was best for me since the beginning.

I am also using this opportunity to express my gratitude to all, the School of Mathematical and Statistical science's faculties and staffs at Clemson who have been so kind and supportive throughout my graduate life. I would like to specially thank my committee members Dr. Hyesuk Lee and Dr. Shitao Liu for their valuable time and support.

Heartiest thanks to our research group members, Dr. Taufiquar Khan (Chair), Sanwar Ahmad, Matthew Brinckerhoff, Shyla Kupis, Lee Redfearn, Scott Scruggs, Thanh To, for their inspiring guidance, invaluable constructive criticism and friendly advice at our research group meetings. Also, I would like to give a special thanks to Shyla Kupis for helping to review this thesis.

A special thanks to all the Bangladeshi Community members at Clemson who

supported me from the beginning of my stay here, encouraged me to start the study, and helped me in many ways.

I always believe from my heart that, there have always been my parents who are praying for me from heaven. I wish, they were here with me today. But, I am lucky enough to have my parents-in-law in my life for whom sometimes I forget that my parents are not alive to encourage me in this world. I want to express my very profound gratitude to my elder brother Mohi Uddin Ahmed for providing me with unfailing support and continuous encouragement since my childhood. Also, I want to acknowledge my all the other family members, my only sister and two younger brothers, brothers-in-law, sisters-in-law who never forget to appreciate my single achievement.

And last but certainly not least I would like to thank my beloved husband Sanwar Uddin Ahmad and our only daughter Subah Zareen Tia whose sacrifice and dreams to fulfill my dream bring me here. Sometimes I lose my beliefs, but my husband never stopped believing in me and has been a firm supporter of mine all these years. He is been always there to help me in my academic needs as well as to perform our household activities smoothly. And it's my daughter who sacrificed most, in my entire graduate life. This accomplishment would not have been possible without them.

I know there are many I forgot to thank or thanked inadequately. When I look back at all the people who have touched my life in just these few years of my life, I am overwhelmed. Thanks, Allah again for everything that I have and that I achieved in my life.

Table of Contents

List of Figures

List of Symbols

Ω	Medium or object
$\partial\Omega$	Boundary of Ω
A	Discretization matrix of the weak formulation.
x	Location variable
b_i	Conversion factor
I	Radiative transport variable of interest
t	Time
c	Speed of light
u	Photon density
S	Strength of the source
D	Diffusion coefficient
μ_a	Absorption coefficient
μ_s	Scattering Coefficient
f	Light source
k	Wave length number
g	Measurements
$\frac{\partial u}{\partial n}$	Normal component of the derivative of u
γ_D	Dirichlet trace
γ_N	Neumann trace
γ_R	Robin trace
$\tilde{Q}$	Parameter space
ϵ	Data noise
β	Regularization parameter
$\bar{F}$	Forward Map
π_i	Dimensionless quantity
$\tilde{p}$	Physical law for dimensional quantity
$\tilde{P}$	Physical law for non-dimensional quantity
q	Physical parameters
$\tilde{q}$	Values of optical parameters
$\tilde{q_0}$	Homogeneous background of optical parameters
Θ	Vector of photon density at mesh points

m	Number of dimensional quantity for a physical law
n	Number of fundamental dimension
L	Fundamental dimensions
L_u	Lagrangian with respect to u
L_D	Lagrangian with respect to D
L_λ	Lagrangian with respect to λ
$\tilde{A}$	Dimension Matrix
r	Rank of $\tilde{A}$
a	Left end point of interval
b	Right end point of interval
J	Cost Functional
Q	Location of observation
$\mathcal{L}$	Lagrangian
λ	Vector of Lagrangian parameters
n_f	Number of mesh points for the forward problem
n_I	Number of mesh points for the inverse problem
A	Discretized matrix
$[a, b]$	Ω
p	Number of experiments
D^*	Background distribution of D
$\hat{p}$	Column vector of unknown exponent
$q*$	Optimal Value of optical parameters
$\tilde{n}$	Refractive index of the medium
C	Constant
c_i	Constant
α_D	Step size for D
α_u	Step size for u
α_λ	Step size for λ
q_i	Dimensional quantity
p_i	Exponent of fundamental dimension
g^δ	Noisy measurement
ρ	Constant greater than one
a_i	Scalar coefficient of vector
V	Right hand side vector in the discretized equation
G	$\frac{\partial(Au)}{\partial D}$
K	$\frac{\partial(A^T\lambda)}{\partial D}$
R	$\frac{\partial(G^T\lambda)}{\partial D}$
Φ	Basis functions

Chapter 1

Introduction

Over the last decades, research in the field of bio-medical imaging has expanded a lot. There has been considerable new research development in bio-medical imaging using optical tomography, in particular diffuse optical tomography. Optical imaging/tomography is a technique for non-invasive imaging inside the body, similar to X-ray imaging. But, unlike X-rays, which use ionizing radiation, optical tomography uses low-energy visible or near infra-red light (NIR) and the special properties of photons to obtain detailed images of bodily organs and tissues. A few advantages of optical imaging are the following: (i) the low energy light is non-ionizing and thus not harmful to tissues; (ii) the medical imaging devices cost less than the existing devices; and (iii) the optical parameters are helpful in providing functional rather than anatomical information [1]. As the tissues have different absorption and scattering properties within the wavelength, other imaging techniques fail to distinguish different kinds of soft tissues. Optical tomography uses the absorption and scattering properties, which has the advantage of being able to detect the deformities or abnormalities in soft tissues.

Due to its effectiveness in detecting abnormalities in soft tissues, one of its most im-

portant applications is in breast cancer detection or mammography, where light can penetrate more easily.

However, diffuse optical tomography (DOT) uses lower doses of X-rays than other medical imaging techniques, which causes these X-rays to not easily penetrate the tissues and requires the use of plates to spread the tissue apart by compressing the breasts. Although X-rays have harmful radiation and are expensive, it is considered one of the most useful techniques because of its stability during inversion. Optical tomography, on the other hand, reduces the use of X-rays; however, the inverse problem suffers from ill-posedness, non-uniqueness and instability due to the noise in the data. Overcoming these issues during inversion in optical imaging has posed a major hurdle in the process of making DOT more accessible in practice rather than just attractive in theory. The derivation of the DOT forward model and its boundary conditions has already been established in many existing literature.

The physical behavior of a system for a given set of known input parameters is predicted by solving forward problem of a mathematical model. However, the inverse problem is to predict the input parameters of the physical system by using observed data from the system that is modeled with the given forward problem. Inverse problem appears in a vast number of different major areas, such as medical imaging, geophysics, astronomy, oceanography, weather prediction, non destructive testing, and many more but in most cases suffers from ill-posedness.

Definition 1.1 (Hadamard's definition of well-posed) A problem is well-posed if

(i) a solution exists,

(ii) the solution is unique, and

(iii) the solution depends continuously on the data. If a solution is not well-posed, then it is called ill-posed.

Computed Tomography (CT), widely known as the CT Scan, is another branch of medical imaging. This process uses X-rays to produce 2-d cross sectional images of the body's bones, soft issues, and blood vessels. These images are then stacked to create 3-d models of specific areas within the body. CT imaging is a nice example of a linear inverse problem, but, unfortunately, X-rays can damage body cells, which can actually increase the risk of cancer. Hence, it is desirable to find new non-invasive medical imaging methods for early detection of cancer. In this thesis, we propose DOT as a potential non-invasive alternative to CT imaging [7]. In contrast to CT inverse problem, DOT inverse problems are neither linear nor well-posed, which makes solving the inverse problem more challenging than other medical imaging techniques. The outline of the thesis is as follows. In Chapter 2, we introduce the DOT problem, which contains the analytic setting and framework of the DOT forward and inverse problems; we provide background on the existence and uniqueness of the forward and the inverse problems. In Chapter 3, we use the method of dimensional analysis to develop a scaled version of the 1-d and 2-d DOT models. Here, we consider several cases using constant and variable parameters for the DOT model. In chapter 4, we introduce the variational formulation of the DOT inverse problem, suggest a cost functional for the minimization problem and describe the algorithm for solving the variational approach for the 1-d DOT model. In chapter 5, we compare the solution of the scaled and non-scaled 1-d DOT models, and we also compare the FEM for the regular DOT and dimensionless DOT model. In this chapter, we present the solution to the DOT inverse problem using simulated data. In chapter 6, we conclude with a summary and propose future work for this thesis.

Chapter 2

Diffuse Optical Tomography: Forward and Inverse Formulation

Diffuse Optical Tomography, well-known as DOT, is a method of imaging that uses near infrared light waves to create 3-d pictures of tissues inside the body. In this chapter, we derive the basic setup for the DOT forward and inverse models. We then present an analytic discussion on the existence and uniqueness of an inverse and a forward solution to the DOT model and, hence, show the well-posedness of the forward problem. Finally, we formulate the inverse problem that provides the foundation for the simulations and experimental verification in Chapter 5. These formulations are well-known results that can be found in many references and, for a comprehensive description, see [7, 16, 5].

2.1 Basic Setup of DOT

In optical tomography, an image is constructed by reconstructing the optical parameters, usually the optical scattering and absorption coefficients, within a

medium. These optical parameters are determined by illuminating the medium with a flash of near-infrared light and taking measurements on the surface. Typically this source is laser light in the visible (about 400 to 700 nm) or near infrared range. By "near-infrared", we are referring to wavelengths between 700 and 1000 nanometers (nm) with most experimental techniques usually falling between 700 nm and 850 nm [7].

Basically, DOT is a type of optical tomography that involves imaging the interior of an object in 2-d or 3-d cross sections using optical waves. Biological tissues are a highly scattered medium, so, as the collimated laser beam passes through the tissue, some of the light is absorbed by chromophores (such as hemoglobin, lipid and water) but most of it is scattered. In fact, in the near infrared range, it has been shown that absorption of light by biological tissue is minimized, so it can penetrate up to about 6 cm in breast tissue and about 2 to 3 cm in the brain and joints [11].

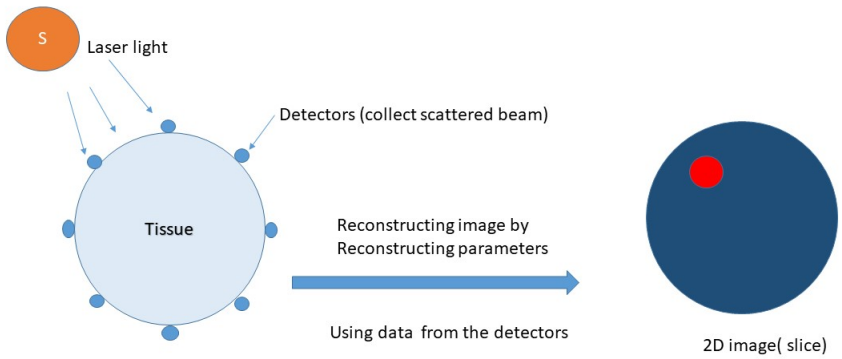

Figure 2.1: Diffuse optical tomography basic set up

The scattered beams are collected at detectors placed on the boundary, and these surface measurements provide a 2-d image (cross-sectional slice) of the object. The

data is used to reconstruct the parameters in the form of a spatial map of the tissue's absorption and scattering coefficients [11] as demonstrated in Figure 2.1. The reduced scattering coefficient is the reciprocal of the the average distance traveled by a photon before its direction is randomized by interaction with another object. The absorption coefficient is the reciprocal of the average distance traveled by a photon before it is absorbed. Usually the tumor cells have higher absorption coefficients than normal cells due to an increased water or ionic concentration. Hence, the absorption and scattering coefficients of the cells being imaged are the most important parameters to be determined in most medical applications [11, 17].

The DOT forward problem will be applied to problems, like breast cancer detection, to determine the measurements, g on the boundary $\partial\Omega$ of the medium Ω given a light source f on the boundary for the given absorption and scattering coefficients μ_a and μ_s. The relationship between these variables is most often described using the radiative transport equation (RTE):

$$\frac{1}{c}\frac{\partial I}{\partial t} + \hat{s}\cdot\nabla I + (\mu_a + \mu_s)I = \mu_s \int p(\hat{s}', \hat{s})I(x, \hat{s}')d\hat{s}', \tag{2.1}$$

where $I(x, \hat{s}, t)$, the variable of interest, is the specific intensity, also known as the spectral radiance (number of photons per unit volume), at position x, in the direction $\hat{s}$ at time t [3, 14].

An approximation to the RTE is usually used since it is computationally expensive and the most common approximation is the diffusion approximation. The model is very well-known as diffuse optical tomography (DOT). In the time domain mode of DOT, the forward problem is expressed using the photon diffusion model

$$-\frac{\tilde{n}}{c}\frac{\partial u(x,t)}{\partial t} + \nabla\cdot D\nabla u(x,t) - \mu_a u(x,t) = -S(x,t), \tag{2.2}$$

where u is the photon density, $\tilde{n}$ is the refractive index of the medium, c is the speed of the light in a vacuum, S is the strength of the source, D is the diffusion coefficient, expressed as $D = \frac{1}{3(\mu_a+\mu_s')}$, where μ_a is the absorption coefficient and μ_s' is the reduced scattering coefficient. The diffusion model is a first order approximation to the RTE, assuming $\mu_s' >> \mu_a$and the detector and source are not too close together [3, 11].

2.2 The DOT Forward Problem

The time independent DOT forward problem involves solving an elliptic partial differential equation with Robin boundary conditions where μ_a and D are known. The solution u describes the photon density of the scattered light arriving at the detectors. The complete DOT experiment is given in the frequency domain by using the Fourier transform as

$$-\nabla \cdot (D\nabla u) + (\mu_a + ik)u = 0 \text{ in } \Omega, \tag{2.3}$$

$$u + 2D\frac{\partial u}{\partial n} = f \text{ on } \partial\Omega, \tag{2.4}$$

$$-D\frac{\partial u}{\partial n} = g \text{ on } \partial\Omega, \tag{2.5}$$

where D is the diffusion coefficient; μ_a is the absorption coefficient; k is the wave number of the modulation frequency of the laser; f is the source; g is a vector of measurements of the scattered photons on the boundary. Here, $\Omega \subset \mathbb{R}^n$, $n = 2, 3$ is assumed to be a bounded, connected Lipschitz domain. Furthermore, in the time independent (DC) case, for $k = 0$, the DOT model is given by

$$-\nabla \cdot D\nabla u + \mu_a u = 0 \text{ in } \Omega. \tag{2.6}$$

Note that D, μ_a, u are all functions of the spatial variable $\mathbf{x}$. Considering D, μ_a are bounded, i.e., there exists constants D_0, D_1 and μ_0, μ_1, such that

$$0 < D_0 \leq D \leq D_1 < \infty, \quad 0 < \mu_0 \leq \mu_a \leq \mu_1 < \infty, \tag{2.7}$$

we can define the parameter space as

$\tilde{Q} := \{(D, \mu_a) \in L^\infty(\Omega) \times L^\infty(\Omega) : 0 < D_0 < D < D_1 \;\; 0 < \mu_0 < \mu_1 < \mu_1\}$.

The Dirichlet trace, Robin trace and the Neumann trace can be defined as the following way, respectively.

$$\begin{aligned} \gamma_D : H^1(\Omega) &\to H^{1/2}(\partial\Omega) \\ u &\longmapsto u|_{\partial\Omega} \end{aligned} \tag{2.8}$$

$$\begin{aligned} \gamma_R : H^1(\Omega) &\to H^{-1/2}(\partial\Omega) \\ u &\longmapsto \left(u + 2D\frac{\partial u}{\partial n}\right)|_{\partial\Omega} \end{aligned} \tag{2.9}$$

$$\begin{aligned} \gamma_N : H^1(\Omega) &\to H^{-1/2}(\partial\Omega) \\ u &\longmapsto -D\frac{\partial u}{\partial n}|_{\partial\Omega} \end{aligned} \tag{2.10}$$

The spaces used above are defined as

$$H^1(\Omega) := \{v \in L^2(\Omega) | \int_\Omega (|\nabla v|^2 + v^2) dx < \infty\}, \tag{2.11}$$

$$H_0^1(\Omega) := \{v \in H^1 | \int_{\partial\Omega} v ds = 0\}, \tag{2.12}$$

$$H^{1/2}(\partial\Omega) \simeq \{\gamma_D(v) | v \in H^1(\Omega)/H_0^1(\Omega)\}, \tag{2.13}$$

$$H^{-1/2}(\partial\Omega) \simeq \{\gamma_N(v) | v \in H^1(\Omega)/H_0^1(\Omega)\}. \tag{2.14}$$

Typically, these spaces are known as Sobolev spaces. The Sobolev space $W_p^k(\Omega)$ is the set of all functions in $L^p(\Omega)$ whose weak partial derivatives are also in $L^p(\Omega)$. Here we are considering $W_2^k(\Omega) = H^k(\Omega)$. Also, $H_0^1(\Omega) \hookrightarrow H^1(\Omega) \hookrightarrow L^2(\Omega)$, $H^{-1/2}(\partial\Omega)$ is the dual space of $H^{1/2}(\partial\Omega)$.

Now, the inner product for the space $H^1(\Omega)$ is

$$\langle u, v \rangle_{H^1(\Omega)} = \int_\Omega (\nabla u \nabla v + uv) dx. \tag{2.15}$$

For DOT measurement, g is considered to be in the Sobolev space $H^{-1/2}(\partial\Omega)$, where the source is also in $H^{-1/2}(\partial\Omega)$ and the photon density is inside the medium in the Sobolev space $H^1(\Omega)$; although, in practice, $L^2(\partial\Omega)$ and $L^2(\Omega)$, respectively, are used in their place [5, 10]. The measurements of g are actually discrete and noisy, so we cannot truly say $g \in H^{-1/2}(\Omega)$ [10]. Thus, this replacement is important, but it has theoretically been shown that for electrical impedance tomography (EIT) and DOT the choice of inner product does make a difference in the reconstruction [10, 12].

Similarly, although the coefficients $D(x)$, $\mu_a(x)$ are generally assumed to be in $L^\infty(\Omega)$, in practice D is considered to be in $H^1(\Omega)$ and $\mu_a \in L^2(\Omega)$ for easier analysis of the uniqueness arguments [5]. In this chapter, we assume $\tilde{Q} \subseteq L^\infty(\Omega) \times L^\infty(\Omega)$ but for inverse problem we restrict the parameter space $\tilde{Q} = H^1(\Omega) \times L^2(\Omega)$. Also, the results

presented here can be extended more generally for $D, \mu_a \in L^p(\Omega)$ and $u \in W^{1,q}$ [5].

To show the first two conditions in definition 1.1 hold, we use the Lax-Milgram theorem for bi-linear forms.

Definition 2.1. (Bi-linear form) A map $B : V \times V \to \mathbb{F}$, where V is a vector space and $\mathbb{F}$ is a field of scalars, is called a bi-linear form if

$$(i) B(a_1u_1 + a_2u_2, v) = a_1B(u_1, v) + a_2B(u_2, v) \text{ and}$$
$$(ii) B(u, a_3v_1 + a_4v_2) = a_3B(u, v_1) + a_4B(u, v_2)$$

where, $u_1, u_2, v_1, v_2 \in V$, $a_1, a_2, a_3, a_4 \in \mathbb{F}$.

Theorem 2.1. (Lax Milgram Theorem):

Let $B : H \times H \to \mathbb{R}$ be a bi-linear form on a Hilbert Space, H and $\langle ., . \rangle$ an inner product. If B satisfies

1. $|B(u, v)| \leq c_1||u||_H||v||_H$ for all $u, v \in H$ and some constant, $c_1 > 0$ (bounded) and

2. $B(u, u) \geq c_2||u||_H^2$ for all $u, \in H$ and some constant $c_2 > 0$, (Coercive)

and if $F(.) : H \to \mathbb{R}$ is a bounded linear functional, then $F(v) \leq c_3||v||_H$.

Then, there exists a unique u, such that $B(u, v) = F(v)$ for all $u, v \in H$.

To obtain the form required in the Lax Milgram Theorem, we find the weak formulation of (2.6). In fact, the weak formulation is necessary to ensure the existence of the required derivatives. That is we can not guarantee the appropriate smoothness of u to guarantee the existence of ∇u and $\nabla \cdot (D\nabla u)$ in the strong sense [5, 6]. We require u to be the Sobolev space $H^1(\Omega)$ in order to guarantee the appropriate smoothness for this weak formulation that is the existence of a derivative of u in $L^2(\Omega)$ [5].

2.2.1 Well-Posedness of the DOT Problem (Robin Boundary Condition)

Here, we are considering the DOT problem which is to solve

$$-\nabla \cdot (D\nabla u) + \mu_a u = 0 \text{ in } \Omega \tag{2.16}$$

$$u + 2D\frac{\partial u}{\partial n} = f \text{ on } \partial\Omega \tag{2.17}$$

for $u \in H^1(\Omega)$. First in order to use Theorem 2.1. we find the weak formulation of the problem.

$$-\int_\Omega (\nabla \cdot (D\nabla u) + \mu_a u)vdx = \int_\Omega 0 \cdot vdx$$

$$\int_\Omega D\nabla u\nabla vdx - \int_{\partial\Omega} D\frac{\partial u}{\partial n}vds + \int_\Omega \mu_a uvdx = 0$$

$$\int_\Omega D\nabla u\nabla vdx + \int_\Omega \mu_a uvdx = \int_{\partial\Omega} \frac{1}{2}(f-u)vds$$

$$\int_\Omega D\nabla u\nabla vdx + \int_\Omega \mu_a uvdx + \int_{\partial\Omega} \frac{1}{2}uvds = \int_{\partial\Omega} \frac{1}{2}fvds$$

through integration by parts and applying the Dirichlet trace (2.8). From the weak formulation we define,

$$B(u,v) = \int_\Omega D\nabla u\nabla vdx + \int_\Omega \mu_a uvdx + \int_{\partial\Omega} \frac{1}{2}uvds \tag{2.18}$$

$$F(v) = \int_{\partial\Omega} \frac{1}{2}fvds. \tag{2.19}$$

To apply theorem 2.1 we need to prove that $B(u,v)$ has a bi-linear form.

Lemma-2.2. $B(u,v)$ is a bi-linear form.

Proof. Let us consider, $u, v, u_1, u_2, v_1, v_2 \in H^1$, $a_1, a_2, a_3, a_4 \in \mathbb{R}$ are scalars.

$$\begin{aligned} B(a_1u_1 + a_2u_2, v) &= \int_\Omega D\nabla(a_1u_1 + a_2u_2)\nabla v dx + \int_\Omega \mu_a(a_1u_1 + a_2u_2)v dx \\ &+ \int_{\partial\Omega} \frac{1}{2}(a_1u_1 + a_2u_2)v ds \\ &= \int_\Omega Da_1\nabla u_1\nabla v dx + \int_\Omega \mu_a a_1u_1 v dx + \int_{\partial\Omega} \frac{1}{2}a_1u_1 v ds \\ &+ \int_\Omega Da_2\nabla u_2\nabla v dx + \int_\Omega \mu_a a_2u_2 v dx + \int_{\partial\Omega} \frac{1}{2}a_2u_2 v ds \\ &= a_1B(u_1, v) + a_2B(u_2, v). \end{aligned}$$

Similarly we can show that

$$B(u, a_3v_1 + a_4v_2) = a_3B(u, v_1) + a_4B(u, v_2)$$

which proves $B(u, v)$ is a bi-linear form.

Next we need to show $B(u, v)$ is bounded and coercive. To make the proof easier, we define a norm that is more intuitive than the H^1 norm to use with our bi-linear form.

Definition 2.2

$$||u||_{H^1_*} = (\int_\Omega (D|\nabla u|^2 + \mu_a|u|^2)dx + \frac{1}{2}\int_{\partial\Omega} |u|^2 ds)^{1/2}. \tag{2.20}$$

Now we will prove the equivalence of this norm to the H^1 norm,

Lemma 2.3. The norms $||u||_{H^1} = (\int_\Omega (|\nabla u|^2 + |u|^2)dx)^{1/2}$ and $||u||_{H^1*}$ are equivalent.

Proof. Recall that, D and μ_a are bounded on Ω, i.e., $D \leq D_1$ and $\mu_a \leq \mu_1$. Let $C_1 = \max_\Omega\{D, \mu_a\}$. Also we are using the fact that for a constant C, $\frac{1}{2}\int_{\partial\Omega} |u|^2 ds \leq$

$C\int_\Omega |\nabla u|^2 + |u|^2 dx$, Then

$$\begin{aligned}
||u||^2_{H^1_*} &= \int_\Omega (D|\nabla u|^2 + \mu_a |u|^2) dx + \frac{1}{2}\int_{\partial\Omega} |u|^2 ds \\
&\leq \int_\Omega (C_1|\nabla u|^2 + C_1|u|^2) dx + \frac{1}{2}\int_{\partial\Omega} |u|^2 ds \\
&\leq C_1 \int_\Omega (|\nabla u|^2 + |u|^2) dx + C\int_\Omega |\nabla u|^2 + |u|^2 dx \\
&= (C_1 + C)||u||_{H^1}
\end{aligned}$$

Next, since $D_0 \leq D$ and $\mu_0 \leq \mu_a$ in Ω,

$$\begin{aligned}
||u||_{H^1} &= \int_\Omega (|\nabla u|^2 + |u|^2) dx \\
&\leq \frac{1}{D_0}\int_\Omega D|\nabla u|^2 dx + \frac{1}{\mu_0}\int_\Omega \mu_a |u|^2 dx \\
&\leq \max\{\frac{1}{D_0}, \frac{1}{\mu_0}\} \left(\int_\Omega (|\nabla u|^2 + |u|^2) dx\right) + \frac{1}{2}\int_{\partial\Omega} |u|^2 ds \\
&\leq \max\{\frac{1}{D_0}, \frac{1}{\mu_0}\} \left(\int_\Omega (|\nabla u|^2 + |u|^2) dx + \frac{1}{2}\int_{\partial\Omega} |u|^2 ds\right) \\
&= C_2||u||_{H^1_*}.
\end{aligned}$$

Thus we have,

$$\frac{1}{C_1 + C}||u||^2_{H^1_*} \leq ||u||_{H^1} \leq C_2||u||_{H^1_*}.$$

Therefore the two norms are equivalent.

Lemma 2.4. $B(u, v)$ is bounded and coercive.

Proof. We use Cauchy-Schwartz inequality to prove $B(u,v)$ is bounded.

$$
\begin{aligned}
|B(u,v)| &= |\int_\Omega D\nabla u\nabla v dx + \int_\Omega \mu_a uv dx + \int_{\partial\Omega}\frac{1}{2}uv ds| \\
&\leq \left(\int_\Omega |D\nabla u|^2 dx\right)^{1/2}\left(\int_\Omega |\nabla v|^2 dx\right)^{1/2} + \left(\int_\Omega |\mu_a u|^2 dx\right)^{1/2}\left(\int_\Omega |v|^2 dx\right)^{1/2} \\
&+ \frac{1}{2}\left(\int_{\partial\Omega}|u|^2 ds\right)^{1/2}\left(\int_{\partial\Omega}|v|^2 ds\right)^{1/2} \\
&\leq D_1\left(\int_\Omega |\nabla u|^2 dx\right)^{1/2}\left(\int_\Omega |\nabla v|^2 dx\right)^{1/2} + \mu_1\left(\int_\Omega |u|^2 dx\right)^{1/2}\left(\int_\Omega |v|^2 dx\right)^{1/2} \\
&+ C\left(\int_{\partial\Omega}|u|^2 ds\right)^{1/2}\left(\int_{\partial\Omega}|v|^2 ds\right)^{1/2} \\
&\leq D_1\left(\int_\Omega |\nabla u|^2 + |u|^2 dx\right)^{1/2}\left(\int_\Omega |\nabla v|^2 + |v|^2 dx\right)^{1/2} + \mu_1\left(\int_\Omega |\nabla u|^2 + |u|^2 dx\right)^{1/2} \\
&\left(\int_\Omega |\nabla v|^2 + |v|^2 dx\right)^{1/2} + C\left(\int_{\partial\Omega} |\nabla u|^2 + |u|^2 dx\right)^{1/2}\left(\int_{\partial\Omega} |\nabla v|^2 + |v|^2 dx\right)^{1/2} \\
&= (D_1 + \mu_1 + C)\left(\int_\Omega |\nabla u|^2 + |u|^2 dx\right)^{1/2}\left(\int_\Omega |\nabla v|^2 + |v|^2 dx\right)^{1/2} \\
&= (D_1 + \mu_1 + C)||u||_{H^1}||v||_{H^1}.
\end{aligned}
$$

Thus $B(u,v)$ continuous if $D, \mu_a \in L^\infty$. Next, by using Lemma 2.3 we prove coercivity.

$$
\begin{aligned}
|B(u,u)| &= |\int_\Omega D\nabla u^2 dx + \int_\Omega \mu_a^2 dx + \int_{\partial\Omega}\frac{1}{2}u ds| \\
&= ||u||^2_{H^1_*(\Omega)} \\
&\geq \frac{1}{C_2}||u||_{H^1}.
\end{aligned}
$$

Then we need to show $F(v)$ is a bounded functional of v. Since we have chosen a closed and bounded domain for our work, it is obvious that $F(v)$ is bounded.
Thus, we have shown all the conditions of Theorem (2.1) are satisfied, so we can

conclude that there exists a unique solution u to the DOT forward model. It can be shown that the third condition of Definition 1.1 is also satisfied, i.e. the solution depends continuously on the data [7, 3], so we can conclude that DOT forward problem is well-posed.

2.3 Analytical Formulation of the Inverse Problem

We encounter inverse problems in many ways in our daily life. For example, while buying fruits from a grocery shop, we try to pick the best product looking at it from outside, i.e., the boundary data, and then we analyze it before deciding which one to pick. Inverse problems, therefore, are important because of their various forms of application. A general inverse problem can be represented mathematically with the equation $F(x) = y$, where the output y is known as well as the transformation function F, but the input data x are unknown. If F has an inverse, such problems are relatively straight forward to solve. However, we know the inverse often does not exist or can only be approximated numerically. In addition, these approximations are very unstable, which can lead to a large change in the output from a small change in the parameters. Thus, inverse problems are often sensitive and do not depend continuously on the data, thereby violating the third condition of Hadamard (see Definition 1.1) and resulting in ill posed problems.

Medical imaging is a natural application of inverse problems as the unknown parameters are the geometry and physiological properties of the tissue being imaged. In the case of optical imaging, like DOT, the "output data" y is the data about the scattered photons read by the detectors at the boundary of the tissue. Due to the sensitivity of the unknown parameter values to small perturbations in the data measurements at the boundary, this problem is ill posed and can only be solved through numerical op-

timization. Furthermore, due to sensitivity of the solution, regularization is needed. Here we will discuss, analyze, and solve the inverse problem for DOT.

2.3.1 The DOT Inverse Problem

In the time independent case, also known as the DC case, the model can be represented as

$$-\nabla \cdot D\nabla u + \mu_a u = 0 \quad \text{in } \Omega, \tag{2.21}$$

$$u + 2D\frac{\partial u}{\partial n} = f \quad \text{on } \partial\Omega. \tag{2.22}$$

It has been shown that the unique recovery of the diffusion and absorption coefficients cannot occur simultaneously [2].

The inverse problem involves estimating the unknown optical parameters, D and μ_a, and reconstructing a spatial map of given by boundary data of the scattered photons collected at the detectors. The DOT inverse problem can be stated as follows: given data g on $\partial\Omega$, find (D, μ_a). Thus, if $\tilde{F}(\tilde{q})$ is the forward operator and g are measurements, then we wish to find $\tilde{q} = (D, \mu_a)$, such that $\tilde{F}(\tilde{q}) = g$, $||\tilde{F} - g^\delta|| \leq \delta$ and g^δ is the vector of perturbed measurements from the data given by

$$g^\delta = \gamma_N \tilde{F}(q*) + \epsilon,$$

where γ_N is the Neumann trace; $q*$ are the true optional parameters; ϵ is the data noise; and, δ is an upper bound on the noise. Experimentally, this problem is ill-posed for a finite data set since it is an under-determined system. Now, $\tilde{q}$ is denoted as the values of optical parameters (D, μ_a), and $\tilde{q}_0$ is denoted as their values on a homogeneous background (D_0, μ_0) as their values on a homogeneous background, such

as healthy tissue. Thus, the image reconstruction problem is to determine $\tilde{q}$ knowing the complete Robin to Neumann map given by

$$-\nabla \cdot (D\nabla u) + \mu_a u = 0 \text{ in } \Omega, \tag{2.23}$$

$$u + 2D\frac{du}{dn} = f \text{ on } \partial\Omega, \tag{2.24}$$

$$-D\frac{du}{dn} = g \text{ on } \partial\Omega. \tag{2.25}$$

Reconstruction is done by minimizing the cost functional,

$$min_{\tilde{q}\in\tilde{Q}} J(\tilde{q}) = \frac{1}{2}||\gamma_n \tilde{F}_R(0,f) - g||^2_{L^2(\partial\Omega)} + \beta||\tilde{q} - \tilde{q_0}||^2, \tag{2.26}$$

where $\tilde{F}_R(0,f)$ is forward Robin operator. The second term $\beta||\tilde{q} - \tilde{q_0}||^2$ in the sum is the smoothing term, which helps smooth the final image with regularization parameter β.

2.3.2 Existence and Uniqueness

The inverse problem for DOT is ill-posed because it violates Hadamard's third condition of well-posedness. Experimentally (for the finite case), this is due to the under-determined problem, and theoretically (for the infinite case), the problem is still unstable because of the noise in the data. Since the forward problem of DOT is well-posed, it was sufficient to consider $\tilde{q} \in \tilde{Q}$. Moreover, we also consider $\tilde{q} \in \{H^2(\Omega) \times L^2(\Omega), 0 < D_0 \leq D \leq D_1 < \infty, 0 < \mu_0 \leq \mu_a \leq \mu_1 < \infty\}$, this assumption will bring more smoothness in the parameter space and become useful to prove the uniqueness of the solution to the inverse problem. This existence and uniqueness is thoroughly discussed in [10], so we do not include the details here.

Chapter 3

Dimensional Analysis for DOT

3.1 Dimensional Analysis

Dimensional Analysis, also known as Unit-factor method, is a problem solving method that uses the fact that any number or expression can be multiplied by one without changing it's value. This involves the analysis of the relationships between different physical quantities by identifying their base quantities, such as mass, length, time etc.

In the initial modeling stage of a problem, one of the simple techniques that is useful is the analysis of the relevant quantities and the dimensional relationship among them. For example, oranges cannot equal grapes plus apples; equations must have consistency to them to make a meaningful relationship among the variables. That is, equations must be dimensionally homogeneous. The methods of dimensional analysis have led to important results in determining the nature of physical phenomena, even when the governing equations were not known. This has been especially true in continuum mechanics out of which the general methods of dimensional analysis evolved. The major benefits from formulating a dimensionless equation of a problem are (i) the

formula is independent of the set of units used, and (ii) there are fewer dimensionless quantities than quantities with dimesions; thus, this formulation is economically more efficient.

The method of dimensional analysis is based on Pi theorem, which is stated as follows: if there is a physical law that gives a relation among a certain number of dimensional physical quantities, then there is an equivalent law that can be expressed as a relation among certain dimensionless quantities (often noted by $\pi_1, \pi_2, ...$, and hence the name) [15]. In the early 1990s, E.Buckingham formalized the original method used by Lord Rayleigh and gave a proof of the Pi theorem for special cases.

3.1.1 The Pi Theorem [15]

A physical law

$$\tilde{p}(q_1, q_2, \ldots, q_m) = 0 \tag{3.1}$$

that relates to the m dimensional quantities q_1, q_2, q_3, $\ldots$, q_m is equivalent to another physical law

$$\tilde{P}(\pi_1, \pi_2, \ldots, \pi_k) = 0 \tag{3.2}$$

that relates to k dimensionless quantities $\pi_1, \pi_2, \ldots, \pi_k$ that can be formed from q_1, q_2, q_3, $\ldots$, q_m.

Now let $L_1, L_2, \ldots, L_n (n < m)$ be fundamental dimensions. In general, for some choice of exponents $a_{1i}, a_{2i}, ...a_{ni}$ the dimensions of q_i, denoted by the square bracket

notation $[q_i]$, can be written in terms of the fundamental dimensions as,

$$[q_i] = L_1^{a_{1i}} L_2^{a_{2i}} ..... L_n^{a_{ni}}.$$

Now, if π is a quantity of the form, $[\pi] = q_1^{p_1} q_2^{p_2} ..... q_m^{p_m}$, which is a monomial in the dimensioned quantities. We need to find all exponents for which $[\pi] = 1$, i.e. π is dimensionless.

$$\begin{aligned}
[\pi] &= [q_1]^{p_1} [q_2]^{p_2} ..... [q_m]^{p_m}, \\
&= (L_1^{a_{1i}} L_2^{a_{2i}} ..... L_n^{a_{ni}})^{p_1} ..... (L_1^{a_{1i}} L_2^{a_{2i}} ..... L_n^{a_{ni}})^{p_m}, \\
&= 1.
\end{aligned}$$

The powers of L_i must sum to zero to make the quantity dimensionless, and, thus, we obtain a homogeneous system of n equations in m unknowns $p_1, p_2, p_3, ..., p_m$ given in matrix form by

$$\tilde{A}\hat{p} = 0$$

where,

$$\tilde{A} = \begin{bmatrix} a_{11} & . & . & . & . & a_{1m} \\ a_{21} & . & . & . & . & a_{2m} \\ . & . & . & . & . & . \\ . & . & . & . & . & . \\ a_{n1} & . & . & . & . & a_{nm} \end{bmatrix}$$

$\tilde{A}$ is the $n \times m$ matrix, known as the dimension matrix and $\hat{p} = [p_1, ... p_m]^T$ is a column vector of the unknown exponents. Solving this system, we get the number

of independent solutions $m - r$, where r is the rank of $\tilde{A}$, which follows from a very well-known result of linear algebra. Recall that, the rank of a matrix is the number of linearly independent rows, which is the number of non zero rows when the matrix is reduced to row echelon form. So, the number of independent dimensionless variables that can be formed from $q_1, q_2, ..., q_m$ is $m - r$.

We are assuming (3.1) is unit free in the sense that it is independent of a particular set of units chosen to express the quantities $q_1, q_2, ..., q_m$.

Definition 3.1 Unit free

The physical law (3.1) is unit free if for all choices of real positive numbers $b_1, b_2, ..., b_n$, we have $\tilde{p}(\bar{q_1}, \bar{q_2}, ..., \bar{q_m}) = 0$ if and only if $\tilde{p}(q_1, q_2, ..., q_m) = 0$, where $\bar{q} = b_1^{p_1} b_2^{p_2} .....b_n^{p_n}$.

Thus, finally we can restate Pi theorem by letting

$$\tilde{p}(q_1, q_2, ..., q_m) = 0 \tag{3.3}$$

be a unit free physical law that relates to the dimensional quantity q_1, q_2, q_3, ... , q_m. And, we can let $L_1, L_2, ...L_n (n < m)$ be the fundamental dimensions. If we form a matrix $\tilde{A}$ (dimensional matrix) with rank r, then there exists $m - r$ independent quantities $\pi_1, \pi_2, ...\pi_{m-r}$ that can be formed from q_1, q_2, q_3, ... , q_m, and the physical law is satisfied

$$\tilde{P}(\pi_1, \pi_2, ...\pi_{m-r}) = 0. \tag{3.4}$$

3.1.2 Proof of the Pi Theorem [15]

We will consider two propositions to prove Pi theorem.

(i) There are $(m-r)$ independent dimensionless variables that can be formed from $q_1, q_2, ...q_m$ dimensional quantities, where m is the number of dimensional physical quantity and r is the rank of the dimension matrix $\tilde{A}$.

(ii) If $\pi_1, \pi_2, ...\pi_{m-r}$ are the $m-r$ dimensionless variables, then two physical laws (3.3) and (3.4) are equivalent.

The proof of (i) has been outlined earlier. It makes use of the familiar results in linear algebra that the number of linearly independent solutions of a set of n homogeneous equations in m unknowns is $m-r$, where r is the rank of the coefficient matrix. For example, let π be a dimensionless quantity. Then,

$$\pi = q_1^{p_1} q_2^{p_2} .....q_m^{p_m} \tag{3.5}$$

for some $p_1, p_2, ...p_m$, in terms of the fundamental dimensions $L_1, ...L_n$.

$$\begin{aligned}
\pi &= [q_1]^{p_1}[q_2]^{p_2}.....[q_m]^{p_m} \\
&= (L_1^{a_{1i}} L_2^{a_{2i}} ......L_n^{a_{ni}})^{p_1} (L_1^{a_{1i}} L_2^{a_{2i}} ......L_n^{a_{ni}})^{p_2} .....(L_1^{a_{1i}} L_2^{a_{2i}} ......L_n^{a_{ni}})^{p_m} \\
&= L_1^{(a_{11}p_1 + a_{12}p_2 + ... + a_{1m}p_m)} ....L_n^{(a_{n1}p_1 + a_{n2}p_2 + ... + a_{nm}p_m)}.
\end{aligned}$$

Because $[\pi] = 1$, the exponent vanishes, or

$$\begin{aligned}
a_{11}p_1 + a_{12}p_2 + ... + a_{1m}p_m &= 0, \\
&\vdots \\
a_{n1}p_1 + a_{n2}p_2 + ... + a_{nm}p_m &= 0.
\end{aligned}$$

By the aforementioned theorem in linear algebra, this homogeneous system has exactly $m - r$ independent solutions $[p_1, ...p_m]$ that form a basis for the null-space or kernel of $\tilde{A}$. Each solution gives rise to a dimensionless variables via (3.5). The independence of the dimensionless variables is based on linear algebraic independence. The proof of (ii) makes strong use of the hypothesis that the law is unit free. The argument is difficult to analyze but for particular case it can be made almost transparent.

3.1.3 Characteristic Scales

To formulate a mathematical model another useful tool is scaling. By scaling one can reformulate a problem in terms of new, usually dimensionless variables. This is a very useful procedure, especially when comparisons of the magnitudes of various terms in an equation are made in order to neglect small terms. This idea is particularly crucial in the application of perturbation methods to identify small and large parameters in a problem. Scaling simplifies the problems by reducing the parameters and also identifies what combination of parameters are important. The characteristic quantities are formed by taking combinations of the various dimensional quantities and should be roughly the same order of magnitude of the quantity itself. The model can then be reformulated in terms of the new variables for the both independent and dependent variables. The result will be a model in dimensionless form, where all the variables and parameters in the problem dimensionless. The process is called non-dimensionalization, or scaling a problem.

3.2 Dimensional Analysis of 1-d DOT

3.2.1 One Dimensional Form of DOT Model

1-d form of DOT equation can be written as,

$$-\frac{d}{dx}\left(D\frac{du}{dx}\right)+\mu_a u=0, \tag{3.6}$$

$$u+2D\frac{du}{dx}=f. \tag{3.7}$$

More precisely we can write the equations as

$$-\frac{d}{dx}\left(D\frac{du}{dx}\right)+\mu_a u=0,\ \text{for } a<x<b, \tag{3.8}$$

$$u-2D\frac{du}{dx}=f_1,\ \text{for } x=a, \tag{3.9}$$

$$u+2D\frac{du}{dx}=f_2,\ \text{for } x=b. \tag{3.10}$$

3.2.2 Dimensional Analysis of 1-d DOT

In the one dimensional DOT model, we are considering the model with respect to independent variable x, variable of interest photon density u. Also in the model we have two parameters absorption coefficient μ_a and diffusion coefficient D. For dimensional analysis we can consider a physical law $\tilde{p}$, which relates to four dimensional

quantities x, u, D, μ_a where,

$$\tilde{p}(x, u, D, \mu_a) = 0. \tag{3.11}$$

We are looking for an equivalent physical law that relates to k dimensionless quantities $\pi_1, \pi_2, ...\pi_k$ that can be formed from x, u, D, μ_a. The fundamental dimensions of all of these quantities are:

$$[x] = L,\ [u] = L^{-1},\ [D] = L,\ [\mu_a] = L^{-1}. \tag{3.12}$$

We might proceed as follows: If π is a quantity of the form,

$$[\pi] = x^{p_1} u^{p_2} D^{p_3} {\mu_a}^{p_4}$$

a monomial in the dimensioned quantities, we want to find all exponents p_1, p_2, p_3, p_4 for which π is dimensionless, or $[\pi] = 1$. Then,

$$[\pi] = [x^{p_1}\ u^{p_2}\ D^{p_3}\ \mu_a^{p_4}] = [L^{p_1}\ L^{-p_2}\ L^{p_3}\ L^{-p_4}] = [L^{p_1 - p_2 + p_3 - p_4}]. \tag{3.13}$$

Now, to make π dimensionless, we write, $p_1 - p_2 + p_3 - p_4 = 0$, i.e, $p_1 = p_2 - p_3 + p_4$. Thus we obtain a homogeneous system of four equations,

$$\begin{bmatrix} p_1 \\ p_2 \\ p_3 \\ p_4 \end{bmatrix} = p_2 \begin{bmatrix} 1 \\ 1 \\ 0 \\ 0 \end{bmatrix} + p_3 \begin{bmatrix} -1 \\ 0 \\ 1 \\ 0 \end{bmatrix} + p_4 \begin{bmatrix} 1 \\ 0 \\ 0 \\ 1 \end{bmatrix} \tag{3.14}$$

From this system we have three independent dimensionless variables that can be formed from x, u, D, μ_a ,

$$\pi_1 = xu, \pi_2 = \frac{D}{x}, \pi_3 = x\mu_a.$$

Thus we have the equivalent Physical law of (3.11)

$$\tilde{P}(\pi_1, \pi_2, \pi_3) = 0. \tag{3.15}$$

Scaling: We can re-scale π_1, π_2, π_3 where the new dimensionless variables π_1', π_2' are still form a set of independent quantity, where,

$$\pi_1' = \frac{\pi_1}{\pi_2} = \frac{xu}{x\mu_a} = \frac{u}{\mu_a} \tag{3.16}$$

$$\pi_2' = \frac{1}{\pi_2} = \frac{x}{D} \tag{3.17}$$

and we can re-write the physical law (3.17) as,

$$\tilde{P}(\pi_1', \pi_2') = 0. \tag{3.18}$$

In terms of our original dimensional variable we than express equation (3.18) as,

$$\frac{u}{\mu_a} = h(\pi_2') \tag{3.19}$$

$$\implies u = \mu_a h(\frac{x}{D}) \tag{3.20}$$

$$\implies u = \mu_a h(s) \tag{3.21}$$

where, $s = \frac{x}{D}$ is our new variable of interest.

3.2.3 Dimensionless DOT Model for Constant D, μ_a

Here we are considering both of the parameters D and μ_a as constant for the dimensionless form of DOT model. Now from (3.21) we are calculating the derivatives of u to rewrite original DOT as a dimensionless form,

$$\begin{aligned}
\frac{ds}{dx} &= \frac{1}{D}, \\
\frac{du}{dx} &= \frac{d}{dx}(\mu_a h(s)) = \frac{d}{ds}(\mu_a h(s)).\frac{ds}{dx} = \mu_a \frac{dh}{ds}\left(\frac{1}{D}\right) = \frac{\mu_a}{D}\frac{dh}{ds}, \\
D\frac{du}{dx} &= \mu_a \frac{dh}{ds}, \\
\frac{d}{dx}\left(D\frac{du}{dx}\right) = \mu_a \frac{d}{dx}\left(\frac{dh}{ds}\right) &= \mu_a \frac{d}{ds}\left(\frac{dh}{ds}\right)\frac{ds}{dx} = \frac{\mu_a}{D}\frac{d^2h}{ds^2}.
\end{aligned}$$

Thus equation (3.8) becomes,

$$-\frac{\mu_a}{D}\frac{d^2h}{ds^2} + \mu_a^2 h = 0$$

$$\implies \frac{d^2h}{ds^2} - \mu_a D h = 0 \tag{3.22}$$

with boundary conditions:

$$\mu_a h - 2\mu_a \frac{dh}{ds} = f_1, \text{ for } s = \frac{a}{D}, \tag{3.23}$$

$$\mu_a h + 2\mu_a \frac{dh}{ds} = f_2, \text{ for } s = \frac{b}{D}. \tag{3.24}$$

3.2.4 Dimensionless DOT Model for Constant μ_a, and Variable D

In this section we have tried to find out dimensionless form of original DOT for known μ_a and variable D. Two types of scaling are used here to form a solvable ODE.

Case 1.

First we try with the same scaling that we used for constant parameters, i.e.

$$\pi_1 = xu, \pi_2 = \frac{D}{x}, \pi_3 = x\mu_a.$$

We have from (3.21), $u = \mu_a h(s)$, where, $s = \frac{x}{D}$.

Now we are calculating derivative of s with respect to x, considering D variable

$$\frac{ds}{dx} = \frac{1}{D} - x\frac{1}{D^2}\frac{dD}{dx} = \frac{1}{D} - \frac{x}{D}\frac{1}{D}\frac{dD}{dx} = \frac{1}{D} - \frac{s}{D}\frac{dD}{dx}.$$

Here details derivation of the derivatives are given step by step.

$$\frac{du}{dx} = \frac{d}{dx}(\mu_a h(s)) = \frac{d}{ds}(\mu_a h(s)).\frac{ds}{dx} = \mu_a \frac{dh}{ds}\left(\frac{1}{D} - \frac{s}{D}\frac{dD}{dx}\right) = \mu_a \frac{dh}{ds}\left(\frac{1}{D} - \frac{s}{D}D'\right).$$

Which implies,

$$D\frac{du}{dx} = \mu_a(1 - sD')\frac{dh}{ds}.$$

Thus we have,

$$\begin{aligned}
\frac{d}{dx}\left(D\frac{du}{dx}\right) &= \frac{d}{dx}\left(\mu_a(1-sD')\frac{dh}{ds}\right) \\
&= \frac{d}{ds}\left(\mu_a(1-sD')\frac{dh}{ds}\right)\cdot\frac{ds}{dx} \\
&= \frac{d}{ds}\left(\mu_a(1-sD')\frac{dh}{ds}\right)\cdot\frac{ds}{dx} \\
&= \mu_a(1-sD')\frac{d^2h}{ds^2}\frac{ds}{dx} + \mu_a\frac{dh}{ds}(-D')\frac{ds}{dx} \\
&= \mu_a(1-sD')\left(\frac{1}{D}(1-sD')\frac{d^2h}{ds^2}\right) + \mu_a(-D')\left(\frac{1}{D}-\frac{s}{D}D'\right)\frac{dh}{ds} \\
&= \mu_a(1-sD')\left(\frac{1}{D}(1-sD')\frac{d^2h}{ds^2} - \frac{D'}{D}\frac{dh}{ds}\right)
\end{aligned}$$

finally we can express (3.8) as,

$$-\frac{\mu_a}{D}(1-sD')\left((1-sD')\frac{d^2h}{ds^2} - D'\frac{dh}{ds}\right) + \mu_a^2 h = 0 \tag{3.25}$$

also the boundary conditions (3.9) and (3.10) becomes,

$$\mu_a h - 2\mu_a(1-sD')\frac{dh}{ds} = f_1, \text{ for } s = a/D, \tag{3.26}$$

and

$$\mu_a h + 2\mu_a(1-sD')\frac{dh}{ds} = f_2, \text{ for } s = \frac{b}{D}. \tag{3.27}$$

Thus, our original DOT model can be expressed as the following dimensionless form

$$(1 - sD')\left((1 - sD')\frac{d^2h}{ds^2}\right) - D'\frac{dh}{ds}) - \mu_a Dh = 0, \tag{3.28}$$

$$h - 2(1 - sD')\frac{dh}{ds} = \frac{f_1}{\mu_a} \text{ for } s = \frac{a}{D}, \tag{3.29}$$

$$h + 2(1 - 2sD')\frac{dh}{ds} = \frac{f_2}{\mu_a} \text{ for } s = \frac{b}{D}. \tag{3.30}$$

Case 2.

In this case we are considering a new scaling for dimensionless variables. Using three independent dimensionless variables i.e.,

$$\pi_1 = xu, \pi_2 = \frac{D}{x}, \pi_3 = x\mu_a$$

where, non-dimensional physical law,

$$\tilde{P}(\pi_1, \pi_2, \pi_3) = 0.$$

Scaling: We can re-write π_1, π_2, π_3 in the following way assuring independence of the new variables:

$$\pi_1' = \pi_1\pi_2 = uD \tag{3.31}$$

$$\pi_2' = x\mu_a \tag{3.32}$$

such that

$$\tilde{P}(\pi_1', \pi_2') = 0.$$

Thus we can write,

$$uD = h(\pi_2') \tag{3.33}$$

$$\implies u = \frac{1}{D}h(x\mu_a) \tag{3.34}$$

$$\implies u = \frac{1}{D}h(s) \tag{3.35}$$

where, $s = x\mu_a$,

$$\begin{aligned}
\frac{ds}{dx} &= \mu_a \\
\frac{du}{dx} &= \frac{d}{dx}\left(\frac{1}{D}h(s)\right) = \frac{d}{ds}\left(\frac{1}{D}h(s)\right).\frac{ds}{dx} = \mu_a\frac{d}{ds}\left(\frac{1}{D}h(s)\right) \\
D\frac{du}{dx} &= D\mu_a\frac{d}{ds}\left(\frac{1}{D}h(s)\right) \\
\frac{d}{dx}\left(D\frac{du}{dx}\right) &= \frac{d}{dx}\left(D\mu_a\frac{d}{ds}\left(\frac{1}{D}h(s)\right)\right) = \mu_a^2\frac{d}{ds}\left(D\frac{d}{ds}\left(\frac{1}{D}h(s)\right)\right).
\end{aligned}$$

Thus equation (3.8) becomes,

$$-\mu_a^2\frac{d}{ds}\left(D\frac{d}{ds}\left(\frac{1}{D}h(s)\right)\right) + \frac{\mu_a}{D}h(s) = 0 \tag{3.36}$$

and the boundary conditions (3.9) and (3.10) become,

$$\frac{1}{D}h - 2D\mu_a\frac{d}{ds}\left(\frac{1}{D}h(s)\right) = f_1,\ s = a\mu_a, \tag{3.37}$$

$$\frac{1}{D}h + 2D\mu_a\frac{d}{ds}\left(\frac{1}{D}h(s)\right) = f_2,\ s = b\mu_a. \tag{3.38}$$

We have solved this dimensionless form of DOT using finite element method and the results are discussed in details in chapter 5.

In the following section we derive the dimensionless form of 2-d DOT model.

3.3 Dimensional Analysis of 2-d DOT Model

In this section we have derived the dimensionless form of 2-d DOT equation stated in equation (2.21). In two dimensional DOT model we are considering the model with respect to independent variable x, y and variable of interest is photon density u. Also in the model we have two parameters absorption coefficient μ_a and diffusion coefficient D. For dimensional analysis, we can consider a physical law $\tilde{p}$ which relates to four dimensional quantities x,y u, D, μ_a where,

$$\tilde{p}(x, y, u, D, \mu_a) = 0 \tag{3.39}$$

we are looking for a equivalent physical law that relates to k dimensionless quantities $\pi_1, \pi_2, ...\pi_k$ that can be formed from x,y, u, D, μ_a. And let the fundamental dimensions of this quantities are:

$$[x] = L,\ [y] = L,\ [u] = L^{-2},\ [D] = L,\ [\mu_a] = L^{-1}. \tag{3.40}$$

Now, we might proceed as follows: if π is a quantity of the form,

$$[\pi] = [x^{p_1}\ y^{p_2}\ u^{p_3}\ D^{p_4}\ \mu_a^{p_5}] = [L^{p_1}\ L^{p_2}\ L^{-2p_3}\ L^{p_4}\ L^{-p_5}] = [L^{p_1+p_2-2p_3+p_4-p_5}] \tag{3.41}$$

a monomial in the dimensional quantities, we want to find all exponents p_1, p_2, p_3, p_4, p_5 for which π is dimensionless, or $[\pi] = 1$. Then, for the dimensionless quantity we need,
$p_1 + p_2 - 2p_3 + p_4 - p_5 = 0$,
i.e, $p_1 = -p_2 + 2p_3 - p_4 + p_5$.

Thus we obtain a homogeneous system of five equations

$$\begin{bmatrix} p_1 \\ p_2 \\ p_3 \\ p_4 \\ p_5 \end{bmatrix} = p_2 \begin{bmatrix} -1 \\ 1 \\ 0 \\ 0 \\ 0 \end{bmatrix} + p_3 \begin{bmatrix} 2 \\ 0 \\ 1 \\ 0 \\ 0 \end{bmatrix} + p_4 \begin{bmatrix} -1 \\ 0 \\ 0 \\ 1 \\ 0 \end{bmatrix} + p_5 \begin{bmatrix} 1 \\ 0 \\ 0 \\ 0 \\ 1 \end{bmatrix} \tag{3.42}$$

from this system we have,

$$\pi_1 = \frac{y}{x}, \quad \pi_2 = x^2 u, \quad \pi_3 = \frac{D}{x}, \quad \pi_4 = x\mu_a$$

where,

$$\tilde{P}(\pi_1, \pi_2, \pi_3, \pi_4) = 0. \tag{3.43}$$

Scaling:

$$\pi_1' = \frac{\pi_1}{\pi_3} = \frac{y}{D}$$

$$\pi_2' = \pi_4 = x\mu_a$$

$$\pi_3' = \frac{\pi_2 \pi_3}{\pi_4} = \frac{x^2 u D}{x x \mu_a} = \frac{uD}{\mu_a}.$$

Thus we can rewrite (3.43) as,

$$\pi_3' = h(\pi_1', \pi_2') \tag{3.44}$$

$$\frac{uD}{\mu_a} = h\left(x\mu_a, \frac{y}{D}\right) \tag{3.45}$$

$$u = \frac{\mu_a}{D} h(s_1, s_2) \tag{3.46}$$

where $s_1 = x\mu_a$ and $s_2 = \frac{y}{D}$.

Thus, considering both D and μ_a constant, we have,

$$\frac{\partial s_1}{\partial x} = \mu_a, \frac{\partial s_1}{\partial y} = 0, \frac{\partial s_2}{\partial x} = 0, \frac{\partial s_2}{\partial y} = \frac{1}{D}$$

$$\begin{aligned}
\frac{\partial u}{\partial x} &= \frac{\partial u}{\partial s_1} \cdot \frac{\partial s_1}{\partial x} + \frac{\partial u}{\partial s_2} \cdot \frac{\partial s_2}{\partial x} = \mu_a \frac{\partial u}{\partial s_1} + 0 = \mu_a \frac{\partial u}{\partial s_1} = \mu_a \frac{\partial}{\partial s_1}\left(\frac{\mu_a}{D} h\right) = \frac{\mu_a^2}{D} \frac{\partial h}{\partial s_1}, \\
\frac{\partial u}{\partial y} &= \frac{\partial u}{\partial s_1} \cdot \frac{\partial s_1}{\partial y} + \frac{\partial u}{\partial s_2} \cdot \frac{\partial s_2}{\partial y} = 0 + \frac{1}{D} \frac{\partial u}{\partial s_2} = \frac{1}{D} \frac{\partial u}{\partial s_2} = \frac{1}{D} \frac{\partial}{\partial s_2}\left(\frac{\mu_a}{D} h\right) = \frac{\mu_a}{D^2} \frac{\partial h}{\partial s_2}.
\end{aligned}$$

Thus

$$(D\nabla u) = \left(\mu_a^2 \frac{\partial h}{\partial s_1} \;\; \frac{\mu_a}{D} \frac{\partial h}{\partial s_2}\right). \tag{3.47}$$

Hence

$$\begin{aligned}
\frac{\partial}{\partial x}\left(\mu_a^2 \frac{\partial h}{\partial s_1}\right) &= \frac{\partial}{\partial s_1}\left(\mu_a^2 \frac{\partial h}{\partial s_1}\right) \cdot \frac{\partial s_1}{\partial x} + 0 = \mu_a^2 \frac{\partial h}{\partial s_1} \mu_a = \mu_a^3 \frac{\partial^2 h}{\partial s_1^2} \\
\frac{\partial}{\partial y}\left(\frac{\mu_a}{D} \frac{\partial h}{\partial s_2}\right) &= 0 + \frac{\partial}{\partial s_2}\left(\frac{\mu_a}{D} \frac{\partial h}{\partial s_2}\right) \cdot \frac{\partial s_2}{\partial y} = \frac{\mu_a}{D} \frac{\partial^2 h}{\partial s_2^2} \cdot \frac{1}{D} = \frac{\mu_a}{D^2} \frac{\partial^2 h}{\partial s_2^2}.
\end{aligned}$$

Thus we have,

$$\nabla \cdot (D\nabla u) = \mu_a^3 \frac{\partial^2 h}{\partial s_1^2} + \frac{\mu_a}{D^2} \frac{\partial^2 h}{\partial s_2^2}.$$

Finally we can reform our original 2-d DOT as,

$$-\mu_a^3 \frac{\partial^2 h}{\partial s_1^2} - \frac{\mu_a}{D^2} \frac{\partial^2 h}{\partial s_2^2} + \mu_a \frac{\mu_a}{D} h = 0 \tag{3.48}$$

or we rewrite as,

$$D\mu_a^2 \frac{\partial^2 h}{\partial s_1^2} + \frac{1}{D} \frac{\partial^2 h}{\partial s_2^2} - \mu_a h = 0 \tag{3.49}$$

and the boundary condition becomes,

$$\frac{\mu_a}{D} h + 2 \left(\mu_a^2 \frac{\partial h}{\partial s_1}, \ \frac{\mu_a}{D} \frac{\partial h}{\partial s_2} \right) \cdot \hat{n}(s_1, s_2) = f. \tag{3.50}$$

Chapter 4

Variational Approach of DOT

The inverse problem of DOT is to recover the parameters from observed optical properties represent a major computational challenge. Most of the traditional strategies employing Gauss-Newton method are computationally slow, mostly due to the formulation and inversion of a large sensitivity matrices. Variational approach using constraint is a good approach to overcome the model error and adaptive inversion using refinement. The inverse problem is formulated as constrained nonlinear optimization problem in [8, 9] by directly working with the governing differential equation. In this chapter, we briefly discuss and reformulate the 1-d DOT inverse problem as constrained optimization problem. To validate the method, numerical results are also presented.

4.1 General Setup

Consider any model ,

$$\bar{F}(D, u) = 0$$

where D is a parameter and u is the variable of interest. We want to recover the parameter D based on observations u which is related to D by a forward model, $\bar{F}$, which after weak formulation in a discretized form can be written as,

$$A(u) = V$$

where A is a square, nonsingular matrix. and V is the right hand side vector.
Denoting the data vector by z and the location of the observations by Q, the problem is to find D such that the above equation holds and

$$||Qu - z|| \leq Tol \tag{4.1}$$

where Tol depends on the noise level. Due to the noisy data and ill-posedness of the inverse problem, there is no unique model which generates the data. Therefore regularization is introduced and a nearby well-posed problem is solved to recover a stable and relatively smooth solution which is unique, at least locally. In practice, we reconstruct D by minimizing the the following least squares residual vector where a regularization term is added,

$$\begin{aligned} J(D, \beta) &= \frac{1}{2}||Qu - z||^2 + \frac{\beta}{2}||W(D - D^*)||^2 \\ \text{s.t. } \bar{F}(D, u) &= 0 \end{aligned} \tag{4.2}$$

where $\beta > 0$ is the regularization parameter, D^* is the background distribution of D and W is a weighing matrix usually the identity matrix.
The problem (4.2) is a nonlinear constraint optimization problem. Thus the con-

strained optimization problem can be rewritten as,

$$J(D,\beta) = \frac{1}{2}||Qu - z||^2 + \frac{\beta}{2}||W(D - D^*)||^2, \tag{4.3}$$
$$\text{s.t. } A(D)u = V.$$

Introducing the Lagrangian,

$$\mathcal{L}(u, D, \lambda) = \frac{1}{2}||Qu - z||^2 + \frac{\beta}{2}||W(D - D^*)||^2 + \lambda^T[A(D)u - V] \tag{4.4}$$

where λ is a vector of Lagrange multipliers. By first order necessary condition at optimality we have,

$$L_u = Q^T(Qu - z) + A^T\lambda \qquad = 0 \tag{4.5}$$
$$L_D = \beta W^T W(D - D^*) + G^T\lambda \qquad = 0 \tag{4.6}$$
$$L_\lambda = Au - V \qquad = 0 \tag{4.7}$$

where $G = \frac{\partial(Au)}{\partial D}$. We consider Newton's method for solving the system. At a given iteration u, D, λ, the Newton correction directions $\delta u, \delta D, \delta\lambda$ are given by,

$$\begin{pmatrix} Q^TQ & K & A^T \\ K^T & \beta W^TW + R & G^T \\ A & G & 0 \end{pmatrix} \begin{pmatrix} \delta u \\ \delta D \\ \delta\lambda \end{pmatrix} = - \begin{pmatrix} L_u \\ L_D \\ L_\lambda \end{pmatrix} \tag{4.8}$$

where $K = K(D,\lambda) = \frac{\partial(A^T\lambda)}{\partial D}$ and $R = R(u, D, \lambda) = \frac{\partial(G^T\lambda)}{\partial D}$. Updated iterations are: $u \mapsto u + \alpha_u\delta u$, $D \mapsto D + \alpha_D\delta D$, $\lambda \mapsto \lambda + \alpha_\lambda\delta\lambda$, and $0 < \alpha_u, \alpha_D, \alpha_\lambda < 1$ are the step sizes determined by line search method.

In next section, we formulate the 1-d DOT problem with a known absorption coeffi-

cient μ_a in the above setting to reconstruct the diffusion coefficient D.

4.2 1-d DOT Model

Consider the 1-d DOT problem (3.8) − (3.10), Multiplying any $v \in H^1[a,b]$ with (3.8) and integrating over $[a,b]$, we have

$$-\int_a^b \frac{d}{dx}\left(D\frac{du}{dx}\right)vdx + \int_a^b \mu_a uvdx = 0$$

Using integration by parts we have,

$$\left(D\frac{du}{dx}v\right)_a^b + \int_a^b Du'v'dx + \mu_a\int_a^b uvdx = 0$$

Using the boundary conditions, we get the weak formulation of 1D DOT as,

$$\int_a^b Du'v'dx + \mu_a\int_a^b uvdx + \frac{1}{2}u(a)v(a) + \frac{1}{2}u(b)v(b) = \frac{1}{2}f_1v(a) + \frac{1}{2}f_2v(b)$$

4.2.1 Finite Element Discretization

Let n_f be the number of mesh points of $[a,b]$, with $x_1 = a < x_2 < ... < x_{n_f} = b$ and $\{\Phi_i(x)\}_{i=1}^{n_f}$ be the set of basis functions such that $\Phi_i(x_j) = \delta_{ij}$.
Thus $u(x) = \sum_{i=1}^{n_f}\Theta_i\Phi_i(x)$, then setting $v = \Phi_j(x)$ in the weak formulation we get a system of linear equation in matrix form :

$$\mathbf{A}\Theta = V \tag{4.9}$$

where,

$$\Theta = (\theta_1, \theta_2, ...\theta_{n_f})^T$$
$$V(j) = \frac{1}{2} f_1 \Phi_j(a) + \frac{1}{2} f_2 \Phi_j(b), \text{ for } j = 1, ..., n_f$$
$$A(i,j) = \int_a^b D\Phi_i' \Phi_j' dx + \mu_a \int_a^b \Phi_i \Phi_j dx + \frac{1}{2}\Phi_i(a)\Phi_j(a) + \frac{1}{2}\Phi_i(b)\Phi_j(b)$$

where $i, j = 1, ..., n_f$.

4.3 Formulation

In order to avoid the inverse crime, we redescritized Ω into $n_I < n_f$ number of mesh points. To solve the inverse problem, the photon density u is measured for multiple experiments. Suppose, p number of experiments are performed and the Neumann data $D\frac{du}{dn}$ at $x = a$ and $x = b$ are measured for each experiment. The Neumann data at the boundary is, $(D\frac{\partial u}{\partial n}(x_i))_{i=\{1,n_I\}}^T = (\frac{u(a)-f_1^l}{2}, -\frac{(u(b)-f_2^l)}{2})^T = Q(u - f^l)$, using the boundary conditions $(3.9 - 3.10)$ for the l-th experiment, where Q is the $(2 \times n_I)$ sparse matrix with $Q_{11} = \frac{1}{2}, Q_{2n_I} = -\frac{1}{2}$. Thus the cost functional $J(D, \beta)$ becomes,

$$J(D, \beta) = \frac{1}{2} \sum_{l=1}^{p} ||Q(u - f^l) - z^{f_l}||^2 + \frac{\beta}{2} ||W(D - D^*)||^2 \tag{4.10}$$

Our goal is to minimize the above functional for D that satisfies,

$$A^l u_l = V^l, \text{ for } l = 1, ..., p. \tag{4.11}$$

We compose the following block matrix,

$$A = diag\{A^1, ..., A^p\}$$

where $A^l, l = 1, ..., p$ are the discretized matrix whose elements are given as,

$$A^l_{ij} = \bar{D}_{ij} + \bar{M}_{ij} + \bar{P}_{ij}$$

with,

$$\begin{aligned}
\bar{D}_{ij} &= \int_a^b D\Phi_i'(x)\Phi_j'(x)dx, \\
\bar{M}_{ij} &= \int_a^b \mu_a\Phi_i(x)\Phi_j(x)dx, \\
\bar{P}_{ij} &= \frac{1}{2}[\Phi_i(b)\Phi_j(b) - \Phi_i(a)\Phi_j(a)].
\end{aligned}$$

We approximate the infinite dimensional parameter D with the function,

$$D(x) = \sum_{i=1}^{N} d_k\hat{\Phi}_i(x)$$

where $\hat{\Phi}_i$ are the basis functions may be on a different set of grid points N than the grid points for the basis functions Φ_i. Then D is approximated by the vector,

$$D = (d_1, ..., d_N)^T.$$

Then the Lagrangian function in (4.4) can be written as,

$$\mathcal{L}(D, u, \lambda) = \frac{1}{2}||Q(u - f) - z||^2 + \frac{\beta}{2}||W(D - D^*)||^2 + \sum_{l=1}^{p} \lambda_l^T[A^l(D)u_l - V^l] \quad (4.12)$$

where $\lambda_1, ..., \lambda_p$ are the vector of Lagrange multipliers, the vector u is written as,

$$u = (u_1^T, ..., u_p^T)^T$$

where $u_l, l = 1, ..., p$ is a vector of length n_I and represents the photon density for each of the p experiments. Using the first order necessary conditions at optimality, we have,

$$L_{u_l} = Q^T(Qu - z^l) + A^{l^T}\lambda_l = 0, \text{ for } l = 1, ..., p \tag{4.13}$$

$$L_D = \beta W^T W(D - D^*) + G_l^T \lambda_l = 0, \text{ for } l = 1, ..., p \tag{4.14}$$

$$L_{\lambda_l} = A^l u_l - V_l = 0, \text{ for } l = 1, ..., p \tag{4.15}$$

where $G_l = \frac{\partial A^l(D)}{\partial D} u_l$. The nonlinear system (4.13 - 4.15) can be solved using the Newton's method. At a given iterate u_l, D, λ_l the Newton correction can be obtained by the solution of the following linear system,

$$\begin{pmatrix} \mathcal{Q} & \mathcal{K} & A^T \\ \mathcal{K}^T & \beta W^T W + \mathcal{R} & \mathcal{G}^T \\ A & \mathcal{G} & 0 \end{pmatrix} \begin{pmatrix} \delta u \\ \delta D \\ \delta \lambda \end{pmatrix} = - \begin{pmatrix} L_u \\ L_D \\ L_\lambda \end{pmatrix} \tag{4.16}$$

where $\mathcal{Q} = diag(Q^T Q)$ is the $(n_I p \times n_I p)$ block matrix, $\mathcal{G} = (G_1^T, ..., G_p^T)^T$ is a $(n_I p \times N)$ block matrix, $\mathcal{K} = (K_1^T, ..., K_p^T)^T$ is a $(n_I p \times N)$ block matrix, with $K_l = \frac{\partial (A_l^T \lambda_l)}{\partial D}$, and $\mathcal{R} = \sum_{l=1}^p R_l$ with $R_l = \frac{\partial (G_l^T \lambda_l)}{\partial D}$. We also have, $L_u = (L_{u_1}^T, ..., L_{u_p}^T)^T$ and $L_\lambda = (L_{\lambda_1}^T, ..., L_{\lambda_p}^T)^T$.

4.3.1 Computing the Sensitivity Matrices

Now we derive the discrete sensitivity relations which will be used to construct the linear system of equations (4.16). Using the finite dimensional approximation of $D(x)$ we get,

$$\bar{D_{ij}} = \sum_{m=1}^{N} d_m \bar{D}_{m,ij} \tag{4.17}$$

where,

$$\bar{D}_{m,ij} = \int_a^b \hat{\Phi}_m(x)\Phi_i'(x)\Phi_j'(x)dx. \tag{4.18}$$

Now differentiating (4.11) with respect to d_m and assuming V^l is independent of d_m, we get,

$$A^l \frac{\partial u_l}{\partial d_m} + \frac{\partial A^l}{\partial d_m} u_l = 0.$$

Thus we have,

$$\frac{\partial u_l}{\partial d_m} = -(A^l)^{-1} \frac{\partial A^l}{\partial d_m} u_l, \quad 1 \leq m \leq N \tag{4.19}$$

here, $\frac{\partial A^l}{\partial d_m} = \bar{D}_m$ is the $(n_I \times n_I)$ matrix whose elements are given by $\bar{D}_{m,ij}$ and $\frac{\partial A^l}{\partial d_m} u_l$ represents m-th column of the $(n_I \times n_I)$ matrix G_l, i.e., $G_l = (\frac{\partial A^l}{\partial d_1} u_l, ..., \frac{\partial A^l}{\partial d_N} u_l)$ for $l = 1, ..., p$.

$K_l = \frac{\partial (A^l)^T \lambda_l}{\partial D}$ is a $(n_I \times n_I)$ matrix with m-th column is the partial derivative of K_l with respect to d_m.

Now differentiating j-th column of $G_l = \frac{\partial A^l}{\partial d_j} u_l$ with respect to d_m, we get,

$$\begin{aligned} \frac{\partial G_l}{\partial d_m} &= \frac{\partial^2 A^l}{\partial d_m \partial d_j} u_l + \frac{\partial A^l}{\partial d_j} \frac{\partial u_l}{\partial d_m} \\ &= \frac{\partial A^l}{\partial d_j} \frac{\partial u_l}{\partial d_m} \end{aligned} \tag{4.20}$$

using definition of $\frac{\partial A^l}{\partial d_m} = \bar{D}_m$, we have $\frac{\partial^2 A^l}{\partial d_m \partial d_j} = 0$. Using (4.20), R_l can be easily computed.

4.3.2 Solving KKT System

This system (4.16), also known as the KKT system must be solved at each iteration. From the last block of (4.16), we can write,

$$\delta u = -A^{-1}(\mathcal{L}_\lambda + \mathcal{G}\delta D). \tag{4.21}$$

Substituting δu in the first block of rows gives,

$$\delta\lambda = \left(A^{-T}Q^TQA^{-1}\mathcal{G} - A^{-T}\mathcal{K}\right)\delta D + A^{-T}Q^TQA^{-1}\mathcal{L}_\lambda - A^{-T}\mathcal{L}_u. \tag{4.22}$$

Finally, from the second block rows, we obtain a linear system for δD alone as,

$$C\,\delta D = -y \tag{4.23}$$

where,

$$C = J_c^T J_c + \beta W^T W + R - S - S^T, \tag{4.24}$$

$$J_c = -QA^{-1}\mathcal{G}, \tag{4.25}$$

$$S = \mathcal{K}^T A^{-1}\mathcal{G}, \tag{4.26}$$

$$y = \beta W^T W(D - D^*) + J_c^T(QA^{-1}V - b) - \mathcal{K}^T(u - A^{-1}V). \tag{4.27}$$

Note that, if $\mathcal{K} = R = 0$, then the above method is known as the Gauss-Newton method.

From (4.11) and (4.13), we can write,

$$u_l = (A^l)^{-1}V^l \text{ for } l = 1, ..., p; \tag{4.28}$$

$$\lambda_l = ((A^l)^T)^{-1}Q^T(Qu_l - z^l) \text{ for } l = 1, ..., p. \tag{4.29}$$

These formulas yield alternatives to the use of (4.21) and (4.22), respectively. Using these formulas one can update the parapmeter D in one of the following four ways:

1. Calculate $\delta u, \delta\lambda$ and δD, using (4.21-4.23), and update u, λ and D simultaneously.

2. Calculate δD and δu from (4.23) and (4.21), and update D and u. Then use (4.29) to update λ. It is assumed that (4.29) holds for the initial iterate.

3. Calculate δD and $\delta\lambda$ from (4.23) and (4.22), and update D and λ. Then update u by (4.11). It is assumed that (4.11) holds for the initial iterate.

4. Calculate δD from (4.23) and update D; then update u by (4.11) and λ by (4.29).

In this thesis, we have used the 3rd variant to update D, λ, then u. A numerical experiment for the reconstruction of D is discussed in the next chapter. The algorithm for the parameter reconstruction is also given next:

4.3.3 Algorithm

1: Start with an initial guess for D and λ.
2: Solve the forward problem for u using the current guess of D.
3: **Stop**, if $||Qu - z|| \leq Tol$.
4: Calculate L_u, L_D and L_λ for the current guess of u, D and λ.
5: Calculate the sensitive matrices $\mathcal{G}, \mathcal{K}$ and $\mathcal{R}$ for the current guess of u, D and λ.
6: Construct the system (4.16) and solve for $\delta u, \delta D$ and $\delta\lambda$.
7: Update D and λ.
8: Repeat step 3 - 7.

Chapter 5

Results and Discussion

In this thesis, we consider the 1-d DOT model described in $(3.8) - (3.10)$. In this chapter, we summarize the simulated results that includes the cost functional for the inverse problem with constant D and μ_a, photon density profile u obtained by using FEM and dimensionless equation, and the reconstruction of the profile of the diffusion coefficient D obtained by solving the inverse problem using the method described in the previous chapter. For convenience, this chapter is divided into three sections. In first section, we considered both D and μ_a as constant. To show the existence of the solution of the corresponding inverse problem, the cost functionals, both scaled and non scaled, are plotted. We also verified the FEM solution by comparing with the analytic solution. For the forward FEM solution, Ω is descretized into $n_f = 200$ mesh points. In the following section, we discuss the results considering a non-constant D and a constant μ_a. The reconstruction of the parameter D, obtained by using the variational method, is presented here. All the reconstructions are done using $n_I = 100$ mesh points to avoid the inverse crime. Finally, we presents the reconstructed image of D, where both D and μ_a are considered to be non-constant and compared the solution with that by the Gauss-Newton method.

5.1 Results for Constant D and μ_a

5.1.1 Cost Functional for 1-d DOT Model

For a simple example, we consider the case where D and μ_a are constants. Then (3.8) – (3.10) can be written as,

$$\frac{d^2u}{dx^2} - \frac{\mu_a}{D}u = 0 \text{ in } \Omega = [a, b] \tag{5.1}$$

$$u - 2D\frac{du}{dx} = f_1 \text{ at } x = a \tag{5.2}$$

$$u + 2D\frac{du}{dx} = f_2 \text{ at } x = b$$

(5.1) has the solution of the form,

$$u(x; D, \mu_a) = c_1 e^{-\sqrt{\frac{\mu_a}{D}}x} + c_2 e^{\sqrt{\frac{\mu_a}{D}}x} \tag{5.3}$$

where c_1 and c_2 are obtained, using the boundary conditions (5.2), as

$$c_1 = \frac{f_1(1 - 2\sqrt{\mu_a D})e^{-\sqrt{\mu_a/D}b} - f_2(1 + 2\sqrt{\mu_a D})e^{-\sqrt{\mu_a/D}a}}{(1 - 2\sqrt{\mu_a D})^2 e^{-\sqrt{\mu_a/D}(b-a)} - (1 + 2\sqrt{\mu_a D})^2 e^{\sqrt{\mu_a/D}(b-a)}},$$

$$c_2 = \frac{f_2(1 - 2\sqrt{\mu_a D})e^{\sqrt{\mu_a/D}a} - f_1(1 + 2\sqrt{\mu_a D})e^{\sqrt{\mu_a/D}b}}{(1 - 2\sqrt{\mu_a D})^2 e^{-\sqrt{\mu_a/D}(b-a)} - (1 + 2\sqrt{\mu_a D})^2 e^{\sqrt{\mu_a/D}(b-a)}}.$$

Setting $q^2 = \frac{\mu_a}{D}$, the above solution can be rewritten as,

$$u(x; q) = c_1 e^{-qx} + c_2 e^{qx} \tag{5.4}$$

where c_1 and c_2 become,

$$c_1 = \frac{f_1(1-2Dq)e^{-qb} - f_2(1+2Dq)e^{-qa}}{(1-2Dq)^2e^{-q(b-a)} - (1+2Dq)^2e^{q(b-a)}},$$
$$c_2 = \frac{f_2(1-2Dq)e^{qa} - f_1(1+2Dq)e^{qb}}{(1-2Dq)^2e^{-q(b-a)} - (1+2Dq)^2e^{q(b-a)}}.$$

If we measure $D\frac{du}{dn}$ at $x = a$ and $x = b$, then the inverse problem is to estimate D and q from the parameter to output map given by, in terms of D,

$$Q_u(x;D) = (D\frac{du}{dn}(a,D), D\frac{du}{dn}(b,D))^T$$

and in terms of q,

$$Q_u(x;q) = (D\frac{du}{dn}(a,q), D\frac{du}{dn}(b,q))^T.$$

We plot the cost functions, $J(D)$ and $J(q)$ for a homogeneous background with $\mu_a = 0.012\text{mm}^{-1}$ and $D = 0.33$ mm. We computed the cost functional $J(D) = \frac{1}{2}||Qu(x;D) - z||^2$, over a range of D values within 25 percent of original value range. We also computed, $J(q) = \frac{1}{2}||Qu(x;q) - z||^2$, within 25 percent of original value range. For constant D and μ_a cost function of both scaling and non scaling looks similar.

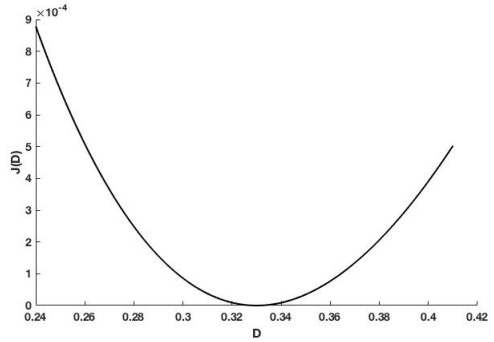

Figure 5.1: Non scaled cost functional $J(D)$, with $\mu_a = 0.012$ and minimum at $D = 0.33$

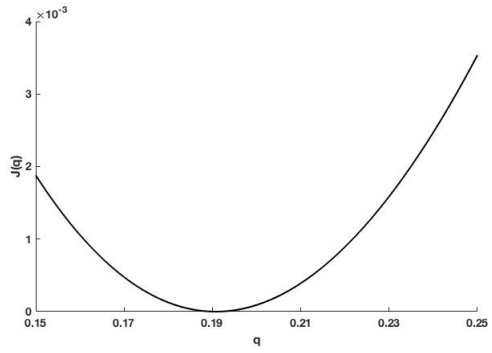

Figure 5.2: Scaled cost functional $J(q)$, with $\mu_a = 0.012$ and $D = 0.33$ and minimum at $q = 0.19$

5.1.2 Comparison of Forward Solution for DOT and Dimensionless DOT Model

In chapter 3, we have derived the dimensionless 1D DOT problem as,

$$\frac{d^2h}{ds^2} - \mu_a D h = 0 \tag{5.5}$$

with boundary conditions,

$$\mu_a h - 2\mu_a \frac{dh}{ds} = f_1, \text{ for } s = \frac{a}{D}, \tag{5.6}$$

$$\mu_a h + 2\mu_a \frac{dh}{ds} = f_2 \text{ for } s = \frac{b}{D}. \tag{5.7}$$

The equation in (5.5) has the solution of the form,

$$h(s) = c_1 e^{\sqrt{\mu_a D}s} + c_2 e^{-\sqrt{\mu_a D}s}. \tag{5.8}$$

Thus, the derivative of h with respect to s is,

$$\frac{dh}{ds} = c_1\sqrt{\mu_a D}e^{\sqrt{\mu_a D}s} - c_2\sqrt{\mu_a D}e^{-\sqrt{\mu_a D}s}. \tag{5.9}$$

from (5.6) and (5.7), we get the following system,

$$\begin{aligned} c_1(1-2\sqrt{\mu_a D})e^{\sqrt{\frac{\mu_a}{D}}a} + c_2(1+2\sqrt{\mu_a D})e^{-\sqrt{\frac{\mu_a}{D}}a} &= \frac{f_1}{\mu_a} \\ c_1(1+2\sqrt{\mu_a D})e^{\sqrt{\frac{\mu_a}{D}}b} + c_2(1-2\sqrt{\mu_a D})e^{-\sqrt{\frac{\mu_a}{D}}b} &= \frac{f_2}{\mu_a} \end{aligned}$$

solving for c_1 and c_2,

$$\mu_a c_1 = \frac{f_1(1-2\sqrt{\mu_a D})e^{-\sqrt{\frac{\mu_a}{D}}b} - f_2(1+2\sqrt{\mu_a D})e^{-\sqrt{\frac{\mu_a}{D}}a}}{(1-2\sqrt{\mu_a D})^2 e^{-\sqrt{\frac{\mu_a}{D}}(b-a)} - (1+2\sqrt{\mu_a D})^2 e^{\sqrt{\frac{\mu_a}{D}}(b-a)}} \tag{5.10}$$

$$\mu_a c_2 = \frac{f_2(1-2\sqrt{\mu_a D})e^{-\sqrt{\frac{\mu_a}{D}}a} - f_1(1+2\sqrt{\mu_a D})e^{-\sqrt{\frac{\mu_a}{D}}b}}{(1-2\sqrt{\mu_a D})^2 e^{-\sqrt{\frac{\mu_a}{D}}(b-a)} - (1+2\sqrt{\mu_a D})^2 e^{\sqrt{\frac{\mu_a}{D}}(b-a)}} \tag{5.11}$$

thus,

$$h(s) = c_1 e^{\sqrt{\mu_a D}s} + c_2 e^{-\sqrt{\mu_a D}s}. \tag{5.12}$$

Applying the scaling defined as $s = \frac{x}{D}$, we get the explicit formula for the electric potential as,

$$u(x) = \mu_a c_1 e^{\sqrt{\frac{\mu_a}{D}}x} + \mu_a c_2 e^{-\sqrt{\frac{\mu_a}{D}}x} \tag{5.13}$$

which is the same solution described in (5.3), as expected.

In this thesis, we solved the one dimensional forward DOT model using finite element method (FEM). For all the numerical computations and simulations, we consider $\Omega = [0, 43]$. Ω is discretized using $n_f = 200$ equally spaced mesh points. In Figure 5.3, we illustrated a comparison of the true solution given by (5.3) and the FEM solution, considering D and μ_a to be constant, and Figure 5.4, demonstrates the validity of the FEM solution.

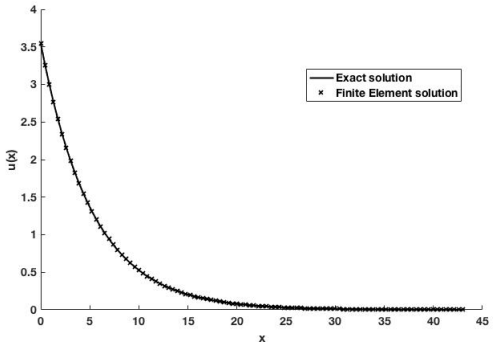

Figure 5.3: Photon density u profile for exact (Both dimensional and non-dimensional) and the FEM solution, for $D = 0.33, \mu_a = 0.012$

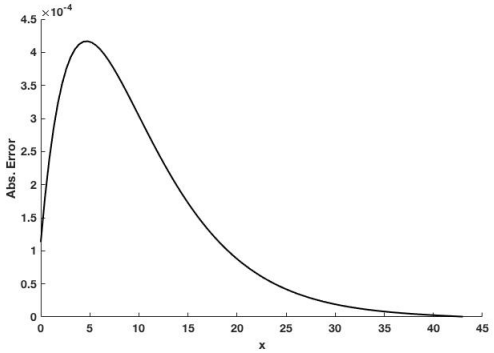

Figure 5.4: Absolute error, |Exact u − FEM u|, for $D = 0.33, \mu_a = 0.012$

5.2 Results for Non-constant D and Constant μ_a

5.2.1 Comparison of the Forward Solutions of Dimensional and Non-dimensional Equation

We have also performed the dimensional analysis for one dimensional DOT model, with variable D and constant μ_a, and formulated the dimensionless DOT model described in $(3.22) - (3.24)$. The diffusion coefficient D is defined as, $D(x) = 0.12$, for $1 \leq x \leq 6$, 0.55 everywhere else, as shown in Figure 5.7. The absorption

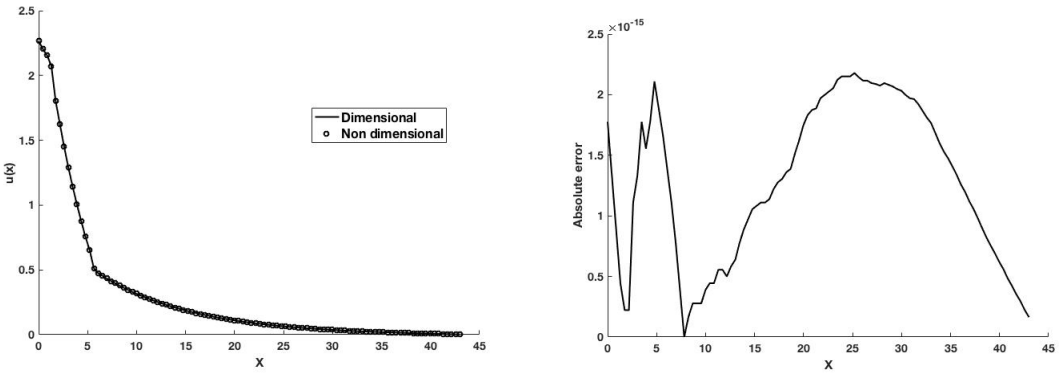

(a) (b)

Figure 5.5: (a) Profile of both dimensional and dimensionless photon density, $u(x)$ obtained by FEM for constant $\mu_a = 0.006$ and variable D, (b) Absolute error between the dimensional and dimensionless solutions

coefficient μ_a is chosen to be constant as 0.006. We set $f_1 = 2.42$ and $f_2 = 0$, for the input.

While choosing the dimensionless scaling described in chapter 4, in case 1, we found that the dimensionless form of the governing equation consists of the term $D' = \frac{dD}{dx}$. Due to this difficulty, we solve the dimensionless forward problem obtained from case 2 using FEM. Figure 5.5(a), illustrates both the profiles of the photon density $u(x)$ obtained from the dimensional and the dimensionless model and figure 5.5(b) shows

the similarity between the dimensional and dimensionless solution. We observe that making the DOT model dimensionless does not have any significant effect to the forward solution.

5.2.2 Reconstruction of D Using Variational Method for Dimensionless and Dimensional DOT Model (μ_a Constant)

We solve the inverse problem for both dimensionless and dimensional 1-d DOT model using variational method. Here, μ_a is considered to be constant, so for the inverse problem, we reconstructed the diffusion coefficient D only. We generate synthetic data for our simulation with the diffusion coefficient D described in Figure 5.7, and absorption coefficient $\mu_a = 0.006$. For a posteriori stopping of the iterations the generalized discrepancy principle, [4, 13], is implemented, i.e., the iterations were stopped at the first index k, for which the residual $||R(D)||^2 = ||Qu(D_k, f) - z||^2$ is less than or equal to $\rho\delta, \rho > 1$.

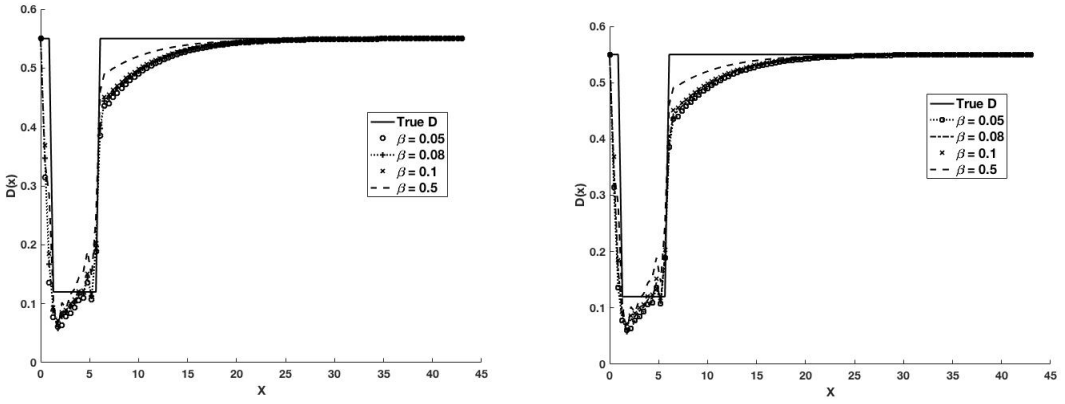

(a) Dimensionless model (b) Dimensional model

Figure 5.6: Reconstructed profile of the diffusion coefficient for different values of β for constant $\mu_a = 0.006$ and variable D

Since the problem is ill-posed, the proper choice of the regularization parameter is

very important for the numerical simulations. Figure 5.6 illustrates the effect of the regularization parameter in the reconstruction of D. For each of the reconstructions, the iteration starts with the natural guess of $D = 0.55$, the background value, and the step size α_D, α_λ both are chosen to be 0.1. In Table 5.1, we summarize the measured

β	Iteration	Relative error	Residual
Dimensionless model			
0.05	8	0.1155	0.0023
0.08	10	0.1051	0.0030
0.1	11	0.0993	0.0035
0.5	20	0.0802	0.0040
Dimensional model			
0.05	8	0.1153	0.0024
0.08	10	0.1051	0.0032
0.1	11	0.0992	0.0036
0.5	20	0.0801	0.0042

Table 5.1: $\alpha_D = 0.1$, $\alpha_\lambda = 0.1$, D non-constant, μ_a constant, $\rho\delta = 5.0E-3$

accuracy in the reconstructions for different values of β. In all the cases, the iterations stops if either the number of iterations exceeds 25 or the residual is less than $\rho\delta = 5.0E-3$. We observe that, the variational method converges faster for lower β, however if β is too small or too large, then the method diverges. For example, in this case, we found that, for $\beta < 0.01$ and for $\beta > 0.5$, the method diverges.

5.3 Results for Non-constant D and μ_a, Dimensional DOT Model

To validate the method for solving the inverse problem described in chapter 4, we solve the inverse problem for 1-d DOT model described in (3.8) − (3.10). For convenience, we reconstructed the diffusion coefficient D only and considered the absorption coefficient μ_a to be known. In this section we discuss the results obtained

for non constant D and μ_a. We had two different discrete diffusion and absorption coefficient inside Ω as, $D = 0.55$ and $\mu_a = 0.006$ in the background and $D = 0.12$, $\mu_a = 0.012$ for $1 \leq x \leq 6$.

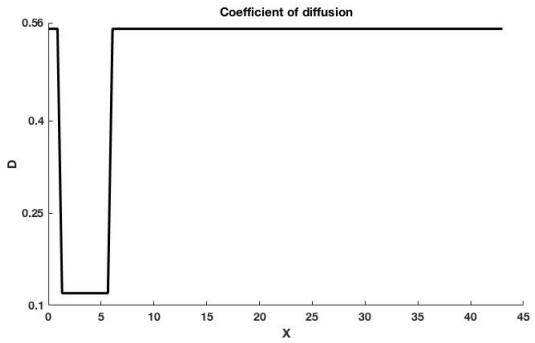

Figure 5.7: Non constant diffusion coefficient D

5.3.1 Reconstruction of D for Different β for Step size $\alpha_D = 0.1$ and $\alpha_D = 0.01$

We observe the effect of the regularization parameter and the step length α_D on the reconstructions.

β	Iteration	$\frac{\|\|D-D_{true}\|\|}{\|\|D_{true}\|\|}$		Residual
		$\|\|\cdot\|\|_2$	$\|\|\cdot\|\|_\infty$	
0.05	6	0.1101	0.7267	0.0034
0.08	8	0.1041	0.7119	0.0035
0.1	9	0.1012	0.6923	0.0037
0.5	18	0.0916	0.5285	0.0039

Table 5.2: $\alpha_D = 0.1$, $\alpha_\lambda = 0.1$, D, μ_a both non-constant, $\rho\delta = 5.0E-3$

In Table 5.2, we summarize the measured accuracy of the reconstructed profiles, that are shown in figure 5.8. Here we choose $\alpha_D = 0.1, \alpha_\lambda = 0.1$ and for each β, the solution obtained before the maximum number of iterations is reached.

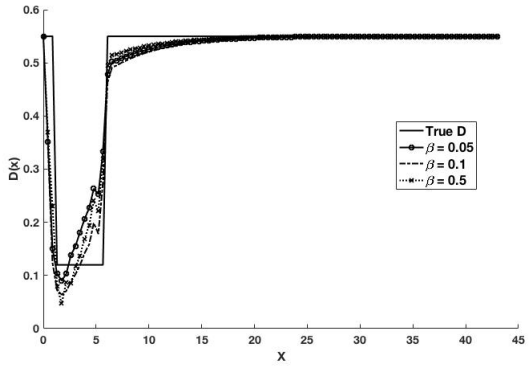

Figure 5.8: Reconstructed D for different β with non constant μ_a and $\alpha_D = 0.1$

To observe the effect of the step length α_D on the reconstruction, we solve the inverse problem for $\alpha_D = 0.01$ and the results are summarized next.

β	Iteration	$\frac{\|\|D-D_{true}\|\|}{\|\|D_{true}\|\|}$		Residual
		$\|\|\cdot\|\|_2$	$\|\|\cdot\|\|_\infty$	
0.05	82	0.1187	0.6584	0.0049
0.08	95	0.1033	0.6254	0.0049
0.1	114	0.1114	0.7095	0.0049
0.5	160	0.0799	0.4486	0.0049

Table 5.3: $\alpha_D = 0.01$, $\alpha_\lambda = 0.1$, D, μ_a both non constant

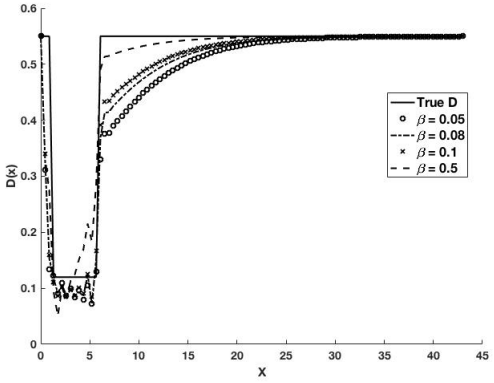

Figure 5.9: Reconstructed D for different β with non-constant μ_a and $\alpha_D = 0.01$

Clearly, for smaller step length, convergence rate gets slower, which is expected. In

both cases, we implemented the generalized discrepancy principle as stopping criterion and chose $\rho\delta = 5.0E-3$. We observe that the reconstructed images of D for different β capture the inclusion better than that of the larger α_D. From Table 5.2 and 5.3, the optimal D is obtained for $\beta = 0.5$, with the minimum relative error in the reconstruction.

As stated earlier, we found that the method converges faster with smaller values of β, but diverges when β is too small or too large.

5.3.2 Convergence in the Reconstruction at Different Iterations

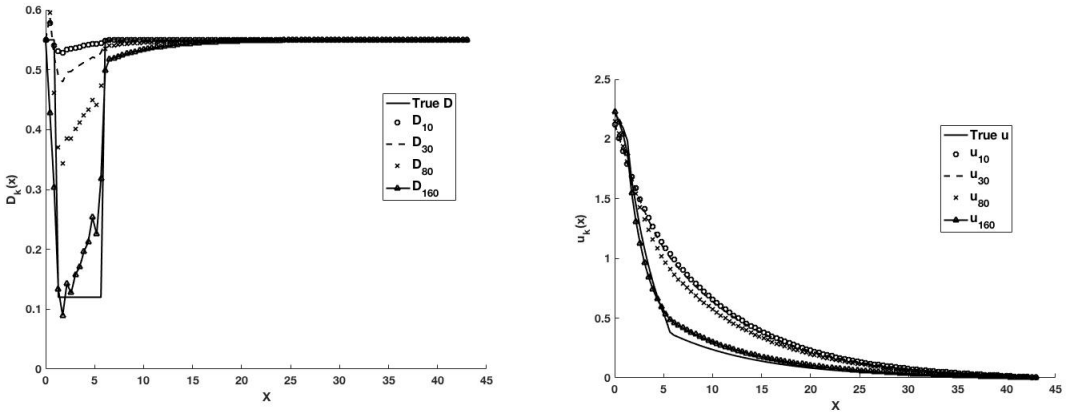

(a) (b)

Figure 5.10: Convergence in the reconstruction of (a) the diffusion coefficient D and (b) photon density $u(x)$, at different iterations for $\beta = 0.5$ and $\alpha_D = 0.01$

Convergence of the reconstruction of D and the photon density profile $u(x)$ are demonstrated in Figure 5.10 at various iterations.

5.3.3 Comparison with Gauss-Newton Approach

We have also compared our results with the classical Gauss-Newton method for nonlinear optimization problem. The inverse solution has a relative error of 0.2468. In compared to the variational method described in this thesis, we can claim that the

variational method produces better reconstruction.

5.3.4 Reconstruction at Different Noise Level

We have also tried adding noise to the simulation, to see the robustness of the variational method. We added 5% and 10% Gaussian noise and noted that the reconstructions are still comparable to that without noise. We chose $\beta = 0.5$ for which we got better reconstruction in noise free setting and to improve the rate of convergence we have chosen $\alpha_D = 0.1$. We observed that, relative error gets higher with the noise level added to the synthetic data.

noise level	Relative error
0%	0.0916
5%	0.0973
10%	0.1190

Table 5.4: Relative error in reconstruction of D at different noise levels, with $\beta = 0.5$, $\alpha_D = 0.1$

5.3.5 Effect of Taking the Inclusion Away from the Endpoints

We have also redefined D and μ_a by taking the inclusion away from the endpoint, e.g. $4 \leq x \leq 10$. However, we noted that, as the inclusion gets away from the endpoints of Ω, the inverse solution loosely capture the inclusion, thus the reconstruction is getting worse.

Chapter 6

Conclusions and Future Work

In this thesis, we described the DOT formulation and provided theoretical justification for well-posedness of both the forward and inverse problem. We formulated the dimensionless form of 1-d and 2-d DOT model. We derived the dimensionless form for constant and variable diffusion coefficient $D(x)$ with μ_a constant. We also discussed the forward and inverse problem in both dimensional and non-dimensional form. We find that scaling does not alleviate the ill-posedness of the problem. We solved the forward problem for both the dimensional and non-dimensional version of the DOT problem using the well-known finite element method. We also used the variational constrained method to formulate the inverse problem in DOT. We devised a numerical algorithm to reconstruct the 1-d diffusion coefficient $D(x)$ by solving the inverse problem as a constrained nonlinear optimization problem. The nonlinear system of equations obtained by applying the first order necessary conditions are solved using Newton's method. The inverse problem using the scaled forward model still suffers from ill-posedness. We investigated the effects of the regularization parameters and the step lengths on the reconstruction. The values of these parameters were chosen so that the algorithm converges as well as to produce a better reconstruction.

We take the most suitable value of the regularization parameter and the step length obtained from noise free data and use them to solve the inverse problem in different noisy environments. We note that the relative error gets higher with the noise level added to the synthetic data. We have also considered the inclusion to be taken inside the body. However, due to the ill-posedness of the problem, the method does not detect the inclusion properly.

The numerical simulations seem to indicate the proposed algorithm regularizes the parameter estimation problem and converge numerically. We used MATLAB for the simulations and numerical computations.

Based on the work presented in this thesis, one can further explore analysis of convergence and stopping criterion of the variational approach, including reconstruction of both D and μ_a with variable μ_a, and extend the algorithm for two and higher dimensional DOT.

Appendices

Appendix A

In this appendix, we provide the MATLAB codes we used for computing the forward solution using finite element method. **MATLAB codes for FEM**

function [sol,K,M,Q,q] = DOTforward(x,DT,muT,sm,h)

n = length(x);

K = zeros(n,n); M = zeros(n,n);

Q = zeros(n,n);

ns = length(sm(1,:));

for i = 1:n-1

zz = linspace(x(i),x(i+1),100);

DD = spline(x,DT,zz);

K(i,i+1) = - trapz(zz,DD)/h^2;

$K(i+1,i) = K(i,i+1);$

end

$for i = 2 : n-1$

$zz1 = linspace(x(i-1), x(i), 100);$

$DD1 = spline(x, DT, zz1);$

$zz2 = linspace(x(i), x(i+1), 100);$

$DD2 = spline(x, DT, zz2);$

$K(i,i) = trapz(zz1, DD1)/h^2 + trapz(zz2, DD2)/h^2;$

end

$zz = linspace(x(1), x(2), 100);$

$DD = spline(x, DT, zz);$

$K(1,1) = trapz(zz, DD)/h^2;$

$Q(1,1) = 0.5;$

$zz = linspace(x(n-1), x(n), 100);$

$DD = spline(x, DT, zz);$

$K(n,n) = trapz(zz, DD)/h^2;$

$Q(n,n) = 0.5;$

$zz = linspace(x(1), x(2), 100);$

$mu = spline(x, muT, zz);$

$mufn = (mu. * (x(2) - zz).^2)/h^2;$

$M(1,1) = trapz(zz, mufn);$

$fori = 1 : n-1$

$zz1 = linspace(x(i), x(i+1), 100);$

$mu1 = spline(x, muT, zz1);$

$mufn1 = (mu1. * (x(i+1) - zz1). * (zz1 - x(i)))/h^2;$

$M(i, i+1) = trapz(zz1, mufn1);$

$M(i+1, i) = M(i, i+1);$

end

for i = 2:n-1

zz1 = linspace(x(i-1),x(i),100);

mu1 = spline(x,muT,zz1);

mufn1 = (mu1.*(zz1-x(i-1)).^2)/h^2;

zz2 = linspace(x(i),x(i+1),100);

mu2 = spline(x,muT,zz2);

mufn2 = mu2.*(x(i+1)-zz2).^2/h^2;

$M(i,i) = trapz(zz1, mufn1) + trapz(zz2, mufn2);$

end

$zz = linspace(x(n-1), x(n), 100);$

$mu = spline(x, muT, zz);$

$mufn = (mu. * (zz - x(n-1)).^2)/h^2;$

$M(n,n) = trapz(zz, mufn);$

F = zeros(n,ns);

for i = 1:ns

F(1,i) = sm(1,i)/2;

F(n,i) = sm(n,i)/2;

end

sol = (K+M+Q);

q = F;

return

Bibliography

[1] Simon R Arridge. Optical tomography in medical imaging. *Inverse problems*, 15(2):R41, 1999.

[2] Simon R Arridge and William RB Lionheart. Nonuniqueness in diffusion-based optical tomography. *Optics letters*, 23(11):882–884, 1998.

[3] Simon R Arridge and John C Schotland. Optical tomography: forward and inverse problems. *Inverse Problems*, 25(12):123010, 2009.

[4] Barbara Blaschke, Andreas Neubauer, and Otmar Scherzer. On convergence rates for the iteratively regularized gauss-newton method. *IMA Journal of Numerical Analysis*, 17(3):421–436, 1997.

[5] John Cooper. Sparsity regularization in diffuse optical tomography. 2012.

[6] E Giusti. Partial differential equations, volume 19, of graduate sudies in mathematics. *American Mathematical Society*, 1998.

[7] Rachel Elizabeth Grotheer. *Hyperspectral Diffuse Optical Tomography Using the Reduced Basis Method and Sparsity Constraints*. PhD thesis, Clemson University, 2016.

[8] Eldad Haber, Uri M Ascher, and Doug Oldenburg. On optimization techniques for solving nonlinear inverse problems. *Inverse problems*, 16(5):1263, 2000.

[9] Kazufumi Ito and Karl Kunisch. The augmented lagrangian method for parameter estimation in elliptic systems. *SIAM Journal on Control and Optimization*, 28(1):113–136, 1990.

[10] Bonnie Jacob. Source optimization in abstract function spaces for maximizing distinguishability: Applications to the optical tomography inverse problem. 2010.

[11] Huabei Jiang. *Diffuse optical tomography: principles and applications*. CRC press, 2010.

[12] Bangti Jin, Taufiquar Khan, Peter Maass, and Michael Pidcock. Function spaces and optimal currents in impedance tomography. *Preprint*, 17, 2009.

[13] T Khan and A Smirnova. 1d inverse problem in diffusion based optical tomography using iteratively regularized gauss–newton algorithm. *Applied mathematics and computation*, 161(1):149–170, 2005.

[14] Taufiquar Khan and A Thomas. Comparison of pn or spherical harmonics approximation for scattering media with spatially varying and spatially constant refractive indices. *Optics communications*, 255(1-3):130–166, 2005.

[15] J David Logan. *Applied mathematics*. John Wiley & Sons, 2013.

[16] Alan Thomas. *Inverse Problems for Partial Differential Equations Arising in Optical Imaging of Highly Scattering Media*. PhD thesis, Clemson University, 2006.

[17] Minghua Xu and Lihong V Wang. Photoacoustic imaging in biomedicine. *Review of scientific instruments*, 77(4):041101, 2006.